Maintaining Two Mating Types: Structure of the Mating Type Locus and Its Role in Heterokaryosis in *Podospora anserina*

Pierre Grognet,*,†,1,2 Frédérique Bidard,†,1,3 Claire Kuchly,†,‡,1,4 Laetitia Chan Ho Tong,*,† Evelyne Coppin,†,‡ Jinane Ait Benkhali,†,‡ Arnaud Couloux,§ Patrick Wincker,§ Robert Debuchy,†,‡ and Philippe Silar*,†,5

*Université Paris Diderot, Sorbonne Paris Cité, Institut des Energies de Demain, 75205 Paris Cedex 13 France, †Université Paris Sud, Institut de Génétique et Microbiologie, Unité Mixte de Recherche 8621, 91405 Orsay Cedex, France, ‡Centre National de la Recherche Scientifique, Institut de Génétique et Microbiologie Unité Mixte de Recherche 8621, 91405 Orsay Cedex, France, §Commissariat a la Énergie Atomique, DSV, IG, Genoscope, 91057 Evry Cedex, France

ABSTRACT Pseudo-homothallism is a reproductive strategy elected by some fungi producing heterokaryotic sexual spores containing genetically different but sexually compatible nuclei. This lifestyle appears as a compromise between true homothallism (self-fertility with predominant inbreeding) and complete heterothallism (with exclusive outcrossing). However, pseudohomothallic species face the problem of maintaining heterokaryotic mycelia to fully benefit from this lifestyle, as homokaryons are self-sterile. Here, we report on the structure of chromosome 1 in *mat*+ and *mat*− isolates of strain S of the pseudohomothallic fungus *Podospora anserina*. Chromosome 1 contains either one of the *mat*+ and *mat*− mating types of *P. anserina*, which is mostly found in nature as a *mat*+/*mat*− heterokaryotic mycelium harboring sexually compatible nuclei. We identified a "*mat*" region ~0.8 Mb long, devoid of meiotic recombination and containing the mating-type idiomorphs, which is a candidate to be involved in the maintenance of the heterokaryotic state, since the S *mat*+ and S *mat*− strains have different physiology that may enable hybrid-vigor-like phenomena in the heterokaryons. The *mat* region contains 229 coding sequences. A total of 687 polymorphisms were detected between the S *mat*+ and S *mat*− chromosomes. Importantly, the *mat* region is colinear between both chromosomes, which calls for an original mechanism of recombination inhibition. Microarray analyses revealed that 10% of the *P. anserina* genes have different transcriptional profiles in S *mat*+ and S *mat*−, in line with their different phenotypes. Finally, we show that the heterokaryotic state is faithfully maintained during mycelium growth of *P. anserina*, yet *mat*+/*mat*+ and *mat*−/*mat*− heterokaryons are as stable as *mat*+/*mat*− ones, evidencing a maintenance of heterokaryosis that does not rely on fitness-enhancing complementation between the S *mat*+ and S *mat*− strains.

A dikaryotic stage during a significant portion of the life-cycle is the hallmark of the higher fungi (*Ascomycota* and *Basidiomycota*), called for this reason the *Dikarya*. The dikaryotic part of the life cycle is different in the two groups. In *Basidiomycota*, mating-competent mycelia fuse and yield the secondary dikaryotic mycelium, upon which basidiospore-bearing dikaryotic fruiting bodies are differentiated. In *Ascomycota*, fruiting bodies are differentiated around a monokaryotic female gametangium (the ascogonium), which is fertilized by a male gamete (antheridium or spermatium) to yield the dikaryon, which undergoes further development and produces numerous ascospore-containing asci. In *Ascomycota*, the dikaryotic stage is thus restricted to the sexual lineage inside the fruiting body. There is one exception to this in the *Taphrinomycetes*, where a dikaryotic mycelium is formed as part of the life cycle (Martin 1940). *Ascomycota* are nonetheless able to exhibit heterokaryotic mycelia following somatic fusion between genetically different individuals (Buller 1933). In *Basidiomycota*, a special structure (the clamp)

doi: 10.1534/genetics.113.159988
Manuscript received November 21, 2013; accepted for publication February 17, 2014; published Early Online February 20, 2014.
Supporting information is available online at http://www.genetics.org/lookup/suppl/doi:10.1534/genetics.113.159988/-/DC1.
Sequence data from this article have been deposited with the GEO Series under accession no. GSE27297.
[1]These authors contributed equally to the work.
[2]Present address: Max Planck Institute for Terrestrial Microbiology, Karl-von-Frisch-Straße 10, D-35043 Marburg, Germany.
[3]Present address: IFPEN, Département Biotechnologie, 1-4 avenue de Bois-Préau, 92852 Rueil Malmaison, France.
[4]Present address: Plateforme Génomique, Génopole Toulouse/Midi-pyrénées, INRA, 24 Chemin de Borde Rouge, Auzeville, CS 52627, 31326 Castanet Tolosan Cedex, France.
[5]Corresponding author: Institut des Energies de Demain (IED), Université Paris Diderot, Sorbonne Paris Cité, Case Courrier 7040, 75205, Paris Cedex 13, France. E-mail: philippe.silar@univ-paris-diderot.fr

enables the maintenance of the dikaryotic state in the mycelium. No such cellular mechanism faithfully maintaining heterokaryosis in mycelia is known in *Ascomycota* (while one exists in the sexual lineage). In the absence of nuclear mixing, mathematical modeling showed that heterokaryotic thalli should often break down into homokaryons (Roper *et al.* 2013).

Pseudohomothallic *Ascomycota*, such as *Podospora anserina* and *Neurospora tetrasperma*, produce *mat+/mat−* (or *mat A/mat a*) dikaryotic ascospores, which upon germination yield a self-fertile heterokaryotic mycelium (Raju and Perkins 1994). In addition to being able to engage in self-reproduction, this mycelium is also able to mate with any partner it may encounter. Moreover, in both species, homokaryotic strains can be obtained from ascospores or, in the case of *N. tetrasperma* from conidia, allowing these organisms to outcross (Dowding 1931; Dodge 1932; Raju 1992). The versatility in breeding behavior probably provides a selective advantage to pseudohomothallism (Billiard *et al.* 2012). Pseudohomothallic ascomycetes therefore unveil interesting questions regarding maintenance of mycelial heterokaryosis in absence of obvious cellular mechanism of nuclear management. In *N. tetrasperma*, different populations produce different levels of homokaryotic conidia, arguing for a genetic regulation of heterokaryosis, affecting the possibility of outcrossing (Corcoran *et al.* 2012). In *P. anserina*, a coprophilous inhabitant of dung, there are no asexual conidia and reproduction is achieved only by sexual reproduction. Ascospores are produced within a fruiting body and are forcibly expelled at maturity. To germinate they need to pass through the digestive track of an herbivore. Homokaryotic ascospores often remain attached with heterokaryotic ones when they are expelled from the fruiting body (Dowding 1931). Under these conditions, loss of heterokaryosis can be mostly achieved during mycelial growth within dung. It is known from previous studies that phenotypic differences exist between the S *mat+* and S *mat−* mycelia of *P. anserina* S strain. For example, S *mat+* and S *mat−* grow at the same rate as S *mat+/mat−*, yet the S *mat−* strain presents a shorter life span than the S *mat+* strain (Marcou 1961), a differential suppression of the *su8-1* suppressor tRNA (Silar *et al.* 2000), triggers the "premature death" syndrome more frequently (Belcour *et al.* 1991) and is slightly more thermoresistant (Contamine *et al.* 2004). More recently, genome-wide microarray analysis revealed that many genes are differentially transcribed in S *mat+* and S *mat−* strains (Bidard *et al.* 2011). Different hypotheses may relate these differences between S *mat+* and S *mat−* strains to the pseudohomothallic lifestyle. It is possible that *mat+/mat−* heterokaryons may be fitter than either one of the *mat+* or *mat−* homokaryons thanks to some genetic complementation between the *mat−* and *mat+* mating types, and thus promoting inbreeding. On the contrary, *mat +/mat−* heterokaryons may rapidly break down because of some incompatibility between the *mat+* and *mat−* mating types, resulting in frequent outbreeding. It is also possible that these differences have no relation to the *P. anserina* lifestyle.

Here, we characterize the mating-type region (*mat*) of *P. anserina* strain S, a large polymorphic region that differentiates the S *mat+* and S *mat−* strains. While the mating-type idiomorphs have been well studied (Picard *et al.* 1991; Debuchy and Coppin 1992; Turgeon and Debuchy 2007), they are embedded in an uncharacterized genomic region devoid of recombination (Marcou *et al.* 1979). The extent of this "*mat* region" is not known, nor are the differences between the two mating types apart from those located at the mating-type idiomorphs and at the *rmp* loci. *rmp* is a gene that has been shown to be polymorphic between the *mat+* and the *mat−* strains in some *P. anserina* isolates and its impact on physiology has been characterized (Contamine *et al.* 2004). By fine genetic mapping and complete sequencing of the *P. anserina* S *mat−* strain and comparison with the previously known sequence of the S *mat+* strain (Espagne *et al.* 2008), we define the borders of the *mat* region and characterize the genetic differences between the two strains. We also identify by microarray analysis the genes differentially expressed between the two strains and whose differential expression does not rely upon the mating-type genes *per se*, but rather on the polymorphic genes present within the *mat* region. Finally, we show that *mat+/mat−* heterokaryotic mycelia are very stable and present evidence that, despite the genetic and phenotypic differences of the S *mat+* and S *mat−* strains, the stability of heterokaryon does not appear to rely on fitness-enhancing complementation.

Materials and Methods

Strains and culture conditions

The strains used in this study derived from the "S" wild-type strain (Rizet and Delannoy 1950). The S *mat+* strain was used for resequencing. Its genome sequence and expressed sequenced tag (EST) are available at http://podospora.igmors.u-psud.fr. Standard culture conditions, media, and genetic methods for *P. anserina* have been described (Rizet and Engelmann 1949; Silar 2013) and the most recent protocols can be accessed at http://podospora.igmors.u-psud.fr/methods.php. Segregation analysis was made with homokaryotic ascospores.

Hygromycin B and phleomycin-resistant strains were obtained by transforming strain S with plasmids derived from pBC-hygro and pBC-phleo (Silar 1995). Primary transformants were crossed with wild type and progeny analysis permitted selection of transgenes segregating independently from the mating type and harboring no phenotypic alteration. In the progeny of these crosses, the same transgenes were associated with either *mat+* or *mat−*.

Construction of the mat− library

DNA from the *P. anserina* S *mat−* strain was extracted as described in Cheeseman *et al.* (2014). The *P. anserina* S *mat−* DNA was nebulized and 1.7 μg of fragmented DNA

was used for library preparation according to the protocol for multiplexed paired-end sequencing of Illumina (part 1005361 RevB, December 2008). Cloning of an aliquot of the library in the pCR4BluntTOPO– (Invitrogen) and analysis of 20 recombinant plasmids indicated that 15 had an insert. Sequencing of 10 inserts indicated that 6 had the upstream and downstream borders required for Illumina multiplex sequencing.

Sequencing

For the resequencing of S *mat+* with the 454 technology, two banks were generated. The first one with 3-kb inserts was sequenced in GsFlex paired reads, generating fivefold coverage. The second bank was used for single Titanium reads generating 17-fold coverage. The combined sequences were assembled with Newbler (software release 2.3-PreRelease-10/19/2009; 454 Life Sciences, Branford, CT). This assembly was colinear with the previous one (Espagne *et al.* 2008) and was used for gap filling and sequencing errors correction using custom-made programs. Accession number is PRJNA12954. For the Illumina sequencing, this work has benefited from the facilities and expertise of the high-throughput sequencing platform of IMAGIF (Centre de Recherche de Gif, http://www.imagif.cnrs.fr). Custom-made libraries had 300-bp inserts and sequencing was 76-bp paired end. For assembly, this work has benefited from the facilities and expertise of the eBio plateforme (IGM, Orsay). Final assembly of the S *mat−* genome was completed with the Velvet program and comparison of S *mat+* and S *mat−* sequences (Zerbino and Birney 2008) with the samtools package (Li *et al.* 2009) and custom-made programs. Accession number for the mat region of the S *mat−* strain is HG934340.

RNA extraction and microarray analysis

Microarray analysis was conducted as previously described (Bidard *et al.* 2010, 2011, 2012). Briefly, four biological replicates for each strain (*mat−*, *mat+*, *fmr1*$^{-}$, and *fpr1*$^{-}$) were grown on minimal medium covered with a cellophane sheet at 27° under constant light for 96 hr. This stage corresponds to fertilization competent mycelium (Bidard *et al.* 2011). Mycelia were harvested by scraping the cellophane surface, frozen in liquid nitrogen and ground in a Mikro-Dismembrator (Sartorius, Göttingen, Germany), and total RNA was purified with the RNeasy Plant Mini Kit (Qiagen, Hilden, Germany). The quality of RNA was controlled on a Bioanalyzed 2100 sytem (Agilent, Santa Clara, CA). One-microgram aliquots of total RNA were amplified and Cy-labeled with Agilent low RNA input fluorescent linear amplification (LRILAK) plus kit and the two-color RNA spike-in kit (Agilent, Santa Clara, CA). The labeling efficiency and the product integrity were checked as described previously (Imbeaud *et al.* 2005). The microarray consisted of a 4 × 44K platform (Agilent) containing 10,556 probes on each array with each probe present in four replicates (Bidard *et al.* 2010). The four biological replicates labeled with Cy-3 for each strain were compared with a common reference labeled with Cy-5, in indirect comparisons. The composition of the common reference was as indicated in Bidard *et al.* (2010). Spot and background intensities were extracted with the Feature Extraction (FE, v. 9.5.3) software (Agilent) using the GE2-v4_95_Feb07 default protocol. FE-software normalized data (Lowess normalized, local background subtracted) were processed with MAnGO (Marisa *et al.* 2007). A moderated *t*-test with adjustment of *P*-value (Benjamini and Hochberg 1995) was computed to measure the significance of each difference of transcript level. Genes were considered as differentially transcribed if *P*-values were <0.005. Data are accessible through GEO Series accession number GSE27297 and Excel files (Supporting Information, Table S3). Fold-changes for each *P. anserina* gene in *mat+ vs. mat−*, *fpr1*$^{-}$ *vs. fmr1*$^{-}$, *mat+ vs. fpr1*$^{-}$, and *mat− vs. fmr1*$^{-}$ comparisons are available from Bidard *et al.* (2011).

Gene deletions

Centromere-like region (CLR) and *Pa_1_18960* were deleted by the split marker techniques as described in Grognet *et al.* (2012). *Pa_1_19950*, *Pa_1_20280*, and *Pa_1_18270* were deleted in S *mat+* and in S *mat−* as described in Bidard *et al.* (2011). Molecular analysis was performed using standard protocols (Ausubel *et al.* 1987) and as in Grognet *et al.* (2012).

In silico analysis

Prediction of mitochondrial or extracellular localization was performed with WoLF PSORT (Horton *et al.* 2007). *P*-values were computed on http://www.graphpad.com/quickcalcs/contingency1.cfm. The figures used for *P*-values computing are shown in Table S1.

Heterokaryon generation and analysis

Heterokaryon were generated by mixing 1 mm^3 explants of the appropriate genotype in 500 μl sterile water with Fastprep FP 120 (MP Biomedicals, Solon-Ohio, Burlingame, CA) at speed 4 for 20 sec. Inoculations were made with 5 μl of the recovered solution at the edge of the petri plates. Under these conditions, heterokaryons formed spontaneously (Silar 2011). For each heterokaryon tested, the experiments were made at least in triplicate at two different times (*e.g.*, a minimum of six plates were tested).

Results

Structure of the P. anserina mat region

As a prerequisite to obtaining an accurate comparison between the *mat+* and *mat−* strains, we resequenced the S *mat+* strain, previously sequenced by the Sanger method (Espagne *et al.* 2008), using the 454 Roche technology with 22-fold coverage and the GA2x technology from Illumina Technology to an 80-fold coverage. Incorporating these data

into the existing assembly enabled us to correct numerous sequencing errors (over 3000), as well as to fill most gaps present in nonrepeated sequences. Finally, the few gaps remaining in nonrepeated sequences were filled manually by sequencing PCR products with extremities unambiguously overlapping gap borders. The S *mat*+ sequence is thus now composed of seven scaffolds representing the seven chromosomes of the nuclear genome, devoid of gaps in unique sequences, and one for the circular mitochondrial chromosome. Missing sequences remain in repeated regions of the nuclear scaffolds, especially at the telomeres and centromeres. Moreover, orientation for two contigs (one at the centromere of chromosome 1 and one at a telomere of chromosome 7) could not be accurately determined because of lack of meiotic recombination, small sizes, and insufficient paired-end sequence data. These contigs are bordered by large regions containing transposons modified by repeat induced point mutation (RIP; Galagan and Selker 2004) and whose sequences are incomplete.

We then sequenced the S *mat*− strain to 65-fold coverage using the GA2x technology from Illumina Technology. The sequence reads were mapped onto the S *mat*+ reference sequence and differences were recorded. The two sequences were identical except on chromosome 1 between nucleotides 6634286 and 7471635, where we could detect 687 polymorphisms: 469 SNP and 218 indels (Table 1). The mating type locus is located within the polymorphic region, identifying this 837,349 bp stretch of DNA as the *mat* region where there is one difference every 1.2 kb in average between the S *mat*+ and S *mat*− strains. This situation was expected as the S *mat*+ and S *mat*− strains are derived from the same wild-type isolate (S) and have been crossed together yearly for the last 60 years and homokaryotic progeny of each mating type was selected for continuing the line. Differences should thus be present only around the mating-type locus in the region devoid of recombination. To check that we correctly identified the borders of the recombination-less region, we genetically mapped several markers with respect to the mating type (Figure 1). The markers were obtained by gene replacements or classical genetics in diverse projects prior to this study (Silar and Picard 1994; Silar *et al.* 1997; Graïa *et al.* 2000; Contamine *et al.* 2004; Bonnet *et al.* 2006; Lambou *et al.* 2008; J. Ait-Benkhali, E. Coppin, and R. Debuchy, unpublished data). Segregation analysis confirmed that no recombination occurred within the *mat* region, whereas recombination could be observed (Figure 1) between the mating type and *Pa_1_17942* ($d = 3.8$ cM, $n = 158$), *Pex5* ($d = 1.7$ cM, $n = 174$), and *Pa_1_21670* ($d = 5.0$ cM, $n = 181$). *Pex5* is located only 50 kb away from the *mat* region defined by sequencing, suggesting a sharp decline of recombination frequency at the border.

The *mat*− region was assembled with Velvet and remaining gaps were manually filled with targeted PCR sequencing. We did not find any large inversion, deletion, or translocation in the *mat* region that could account for the lack of recombination, as all differences, except for the mating-type idiomorph *per se*, affected few contiguous nucleotides. However, in both the *mat*+ and *mat*− strains there is a region located between nucleotides 7258560 and 7266980 containing several transposons modified by RIP and whose sequence is incomplete for both S *mat*+ and S *mat*−. Because this cluster of ripped transposons is reminiscent of a centromere (Talbert and Henikoff 2010), this region was designated as centromere-like region (CLR). Attempts to fill the gaps in both strains by long-range PCR amplification failed, suggesting that CLR was quite large (>20 kb). To ensure that the structures of CLR in both strains are the ones partially described in the assemblies, we replaced them *in vivo* with resistance markers (to nourseothricin in S *mat*− and to hygromycin B in S *mat*+). We were able to obtain both strains (CLR^{Δ} *mat*+ and CLR^{Δ} *mat*−) with the expected replacement (see Figure S1 for Southern blot validation of all replacements made during this study), indicating that the CLR borders defined by sequencing are those actually present in the genome. The *mat*+ and *mat*− chromosome 1 of *P. anserina* are thus totally colinear and have not undergone inversions.

Table 1 Differences in the *mat* region between the *mat*+ and *mat*− strains

Transitions	299	
Transversions	170	
Indels	218	
	Obs	Exp
Intergenic	499	411
Genic intron	35	19
Genic	153	257
Silent	75	50
Nonsilent	78	103

CLR is not involved in repression of recombination in the mat region

Phenotypic analysis of the strains devoid of CLR did not show any obvious phenotypic difference with the wild type. Especially, recombination frequency in the mating-type region remained unchanged, as we could not recombine CLR^{Δ} and *mat* ($d = 0$ cM; $n = 175$). Even in the F5 generation of $CLR^{\Delta} \times CLR^{\Delta}$ crosses, we could not find any recombinant over 180 tested progeny.

Coding differences between the S mat+ and S mat− mat regions

The *mat* regions of S *mat*+ and S *mat*− both contain 229 coding sequences (CDS), as well as the *FPR1* gene in the S *mat*+ strain and the *FMR1*, *SMR1*, and *SMR2* genes in the S *mat*− strain. Polymorphisms were preferentially present in intergenic and intronic sequences (Table 1; χ^2 test; $P < <0.001\%$) and silent polymorphisms were in much excess to the expected value under a model of random accumulation of mutations (Table 1; χ^2 test; $P < <0.001\%$), indicating that nonsilent mutations were counterselected in the

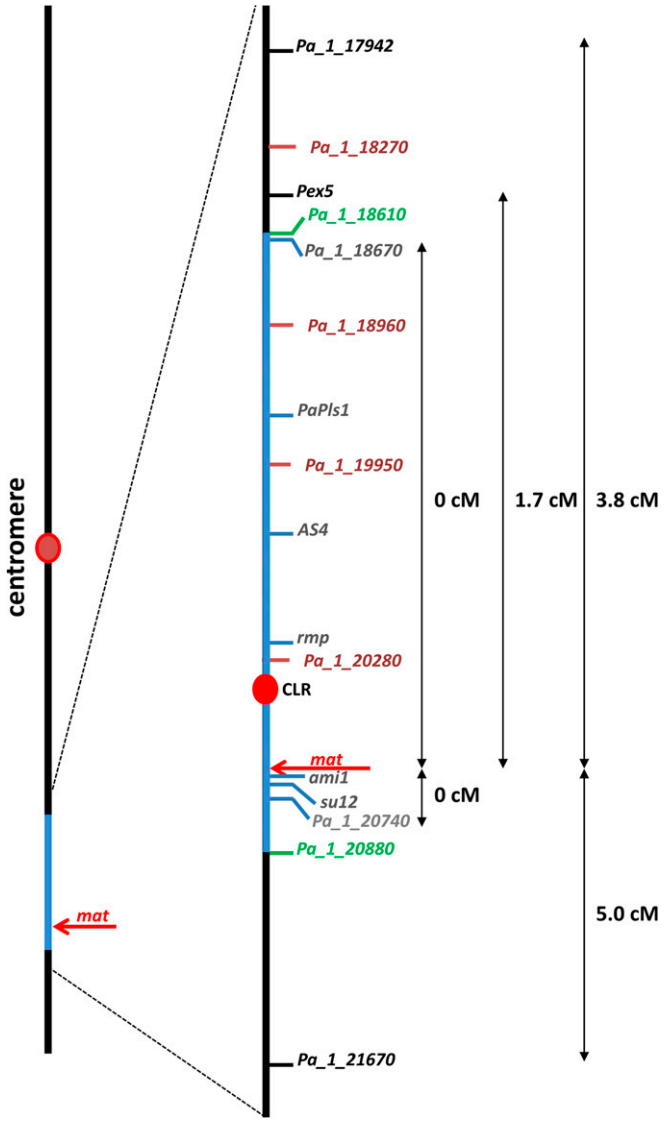

Figure 1 Scheme of chromosome 1 and expansion of the *mat* region (in blue). Key features and CDS are mapped on the diagram. CDS labeled in gray type are tightly linked to the mating type ($d < 0.5$ cM); those in green type are at the borders of the *mat* region.

CDS of *mat* region. We then plotted the distance between each consecutive mutation to see if there is accumulation in some regions and scarcity in others (Figure 2). Data show a rather uniform spacing between mutations along the whole region. However, a few large stretches of DNA were devoid of polymorphisms, especially two 15-kb polymorphism-free sequences that split the *mat* region in three parts of 212, 369, and 246 kb. These two regions show no obvious differences in their coding capacity as compared to the rest of the *mat* region. Mutations are more closely packed toward the telomere end of the *mat* region and there appears to be a few hot spots of polymorphisms, including one around the mating type and the other in the *Pa_1_18960* CDS. This CDS is highly unusual as it is composed of a ≈3000-amino-acid-long region very rich in threonine/serine, bordered by two domains conserved in other Sordariales, such as *Neurospora crassa* and *Chaetomium globosum* (Figure S2). The threonine-/serine-rich domain is similar to those found in yeast agglutinins (Dranginis *et al.* 2007). The conserved *N* terminus contains a predicted signal for peptide secretion as well as three carbohydrate binding domains, strongly suggesting that this agglutinin-like protein is inserted into the cell wall for some unknown purpose. We deleted the *Pa_1_18960* gene in both S *mat*+ and S *mat*− strains and assessed the fertility of the *Pa_1_18960*$^{\Delta}$ deleted strains. We could not see any difference in S *mat*+ × S *mat*− and *Pa_1_18960*$^{\Delta}$ *mat*+ × *Pa_1_18960*$^{\Delta}$ *mat*− crosses after fertilization (*i.e.*, fruiting bodies and ascospores were in the same amounts); however, the mutant produced three times more spermatia than wild type produced. Finally, like for the deletion of CLR, we could not dissociate the *Pa_1_18960*$^{\Delta}$ deletions from the mating types ($n = 61$), indicating that this region is not involved in the repression of recombination in the *mat* region. Intriguingly, three additional CDS-resembling yeast agglutinins are present within the *mat* region (*Pa_1_19950* and *Pa_1_20280*) or very close (*Pa_1_18270*). None are polymorphic between S *mat*+ and S *mat*−. Inactivation of *Pa_1_19950* and *Pa_1_18270* did not result in any obvious phenotype, while inactivation of *Pa_1_20280* resulted in mature perithecia that contained ascospores, yet none were discharged as occurred in the wild type (Figure S3).

Few additional genes contained polymorphisms that would present obvious phenotypic outcome (Table S2). The *rmp1* gene (*Pa_1_20180*) has G/E and STOP/Q polymorphisms (Contamine *et al.* 2004; Table S2) and has previously been shown to account for differences in the timing of the premature death syndrome and thermosensitivity of S *mat*+ and S *mat*−. Large indels are found in *Pa_1_19010*, a CDS of unknown function specific to *P. anserina*, and *Pa_1_20400*, a CDS conserved in some *Ascomycota* and carrying an EOS1 domain involved in sensitivity to high-sucrose stress (Nakamura *et al.* 2007). A polymorphism removes in S *mat*− the predicted start codon of *Pa_1_20750*. However, this CDS is small and specific to *P. anserina*; it may be miscalled a gene. A few other CDS carry polymorphisms in excess of what is expected, indicative of possible positive selection: *Pa_1_19460* (six polymorphisms, three nonsilent) coding a glycoside hydrolase of CAZy family 76, *Pa_1_20560* (three polymorphisms, two nonsilent) coding a putative subunit of the anaphase-promoting complex, *Pa_1_20650* (three nonsilent polymorphisms) coding a putative DNA polymerase zeta subunit, as well as *Pa_1_19040* (five polymorphisms, three nonsilent), *Pa_1_19560* (three nonsilent polymorphisms), and *Pa_1_20140* (four polymorphisms, three nonsilent) coding proteins of unknown function conserved in *Pezizomycotina*. Thirty-nine additional CDS carry polymorphisms with changed coding capacity resulting in polymorphic proteins that can possibly account for phenotypic differences between the S *mat*+ and S *mat*− strains.

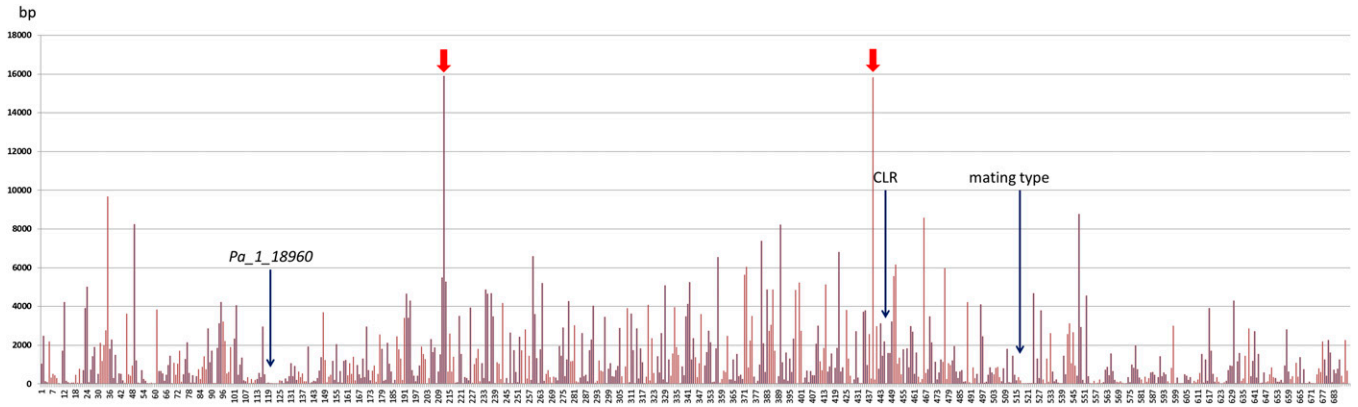

Figure 2 Plot of the distances between each consecutive mutation. The *y*-axis gives the size of the region up to the next mutation for all 687 mutations ordered on the *x*-axis according to their succession on the chromosome starting from the centromere toward the telomere. Red arrows point to two 15-kb regions devoid of polymorphism.

Microarray analysis evidences differences in transcript accumulation between S mat+ and S mat−

To evaluate potential effects of the *mat* region *vs.* the mating type on the physiological differences between the S *mat+* and S *mat−* strains, we identified the genes differentially expressed at the level of transcription between the two strains. Genes specifically regulated by the mating-type genes were previously investigated (Bidard *et al.* 2011). The analysis uncovered 683 genes expressed higher in *mat−* strain and 371 genes expressed higher in *mat+* strains under crossing conditions. These 1054 differentially transcribed genes mapped on all chromosomes, including the mitochondrial one, and there appears to be no preferential clustering in a particular chromosome (χ^2 test; *P*-value > 0.1). The comparison of wild type with *fpr1*$^-$ and *fmr1*$^-$ strains, which have loss-of-function mutations in the mating-type idiomorphs (El-Khoury *et al.* 2008), allowed us to assess the role of the mating-type genes in differential expression and to dissociate their effect from that of the *mat* region (mating-type genes not included). Among the 1054 genes, the vast majority (860 genes) was under the control of the *mat* idiomorphs and only 194 genes were differentially transcribed due to differences between *mat+* and *mat−* strains excluding the *mat* idiomorphs (Figure 3). Among the 194 genes, 131 genes had higher expression in the *mat−* strain, while 63 genes had higher expression in the *mat+* strain (Table S3). Analysis of the functions of the 194 genes revealed consistent differences between S *mat+* and S *mat−*, indicative of metabolic differences between the two strains (Table S4). A total of 21 glycoside hydrolase genes had higher expression in the S *mat−* strain, as well as various other genes involved in carbon metabolism [*e.g. Pa_6_11500* and *Pa_5_1860* (Pec_lyase_C) and *Pa_7_1080* (O-FucT)]. The enrichment in glycoside hydrolases among the 194 genes was highly significant (*P*-value < 0.0001). Strikingly, the set of genes with higher expression in S *mat+* did not contain any gene belonging to this family. As most glycoside hydrolases were expected to be secreted, the S *mat−* highly expressed category was enriched in putative extracellular proteins (*P*-value = 0.0003). The *nad2* and *nad3* mitochondrial genes had high expression in the *mat−* strain, but the genes highly expressed in S *mat+* showed a strong enrichment in nuclear genes encoding proteins with known or predicted mitochondrial localization (*P*-value = 0.0005). A total of 13 nuclear genes encode well-known mitochondrial proteins among the genes with high expression in the *mat+* strain, including three proteins related to the iron–sulfur cluster binding domain. Most of the 194 genes had less than twofold differences between S *mat+* and S *mat−*. In a second analysis, we investigated in more detail 46 genes that were strongly regulated by the *mat* region (*i.e.*, they had a statistically significant twofold or more differences in their expression between S *mat+* and S *mat−*), but that would present little control by the mating type, which had less than twofold differences when S *mat+* (resp. *mat−*) was compared to the *fpr1*$^-$ (resp. *fmr1*$^-$) mutant (Table S5). Only 19 of these genes belonged to the 194 genes not regulated at all by the mating type. None of the 46 selected genes had a fold change above five; most had a two- to threefold change. Intriguingly, among the genes identified in the analysis, 21 have no obvious function that can be deduced from their sequence, 3 encode putative plasma membrane transporters, and 20 encode enzymes involved in various metabolisms, including respiration. One encodes an enzyme involved in the post-translation modification of proteins (*Pa_7_9690*) and one (*Pa_1_30*) is similar to *Aspergillus nidulans TmpA*, a gene encoding an oxidoreductase involved in the production of a metabolite controlling the sexual and asexual cycles (Soid-Raggi *et al.* 2006). Three of the 46 genes are in the *mat* region and two (*Pa_1_19170* and *Pa_1_20140*) are polymorphic between S *mat+* and S *mat−*. Both encode proteins of unknown function. Still, *Pa_1_20140* contains more than expected polymorphisms (four polymorphisms, three nonsilent). The fact that half of the 46 genes were involved in metabolic processes confirms that the physiology of the S *mat+* and S *mat−* strains may be slightly different.

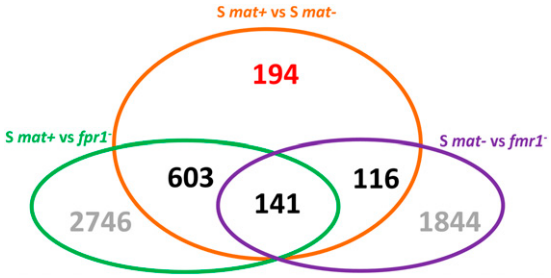

Figure 3 Venn diagram of genes differentially regulated (*P*-value < 0.005) between the S *mat*+ and S *mat*− strains, and S *mat*+ and S *mat*− mating-type mutants, under crossing conditions. Mating-type mutants have loss-of-function mutations in *FPR1* (*mat*+) and *FMR1* (*mat*−) (El-Khoury *et al.* 2008). Orange set: genes differentially expressed in the S *mat*+ *vs.* S *mat*− comparison. Green set: genes differentially expressed in the *mat*+ *vs. fpr1*$^-$ comparison. Violet set: genes differentially expressed in the *mat*− *vs. fmr1*$^-$ comparison. A total of 194 genes are differentially expressed between *mat*+ and *mat*− strains and not controlled by mating-type genes (see Table S3). A total of 141 genes are differentially expressed between *mat*+ and *mat*− strains and controlled by *FMR1* and *FPR1*. A total of 603 and 116 genes are differentially expressed between *mat*+ and *mat*− strains and controlled by *FPR1* and *FMR1*, respectively.

mat+/mat− heterokaryons are stable

To check if S *mat*+/*mat*− heterokaryons had some advantage over S *mat*+ and S *mat*− homokaryons, we measured apical growth and monitor mycelium morphology under various conditions. Growth rate of the heterokaryotic *mat*+/*mat*− cultures was not different from that of homokaryotic *mat*+ or *mat*− cultures on M2 and M0 (M2 lacking dextrin) covered with a layer of cellophane as carbon source, at 18°, 23°, 27°, and 30°; 37° was not assayed as at this temperature S *mat*− and S *mat*+ grew differently (Contamine *et al.* 2004). Moreover, we did not see any obvious morphological differences aside from the presence of perithecia in heterokaryotic cultures. Stability of these S *mat*+/S *mat*− heterokaryons was tested by inoculating heterokaryotic mycelia on various media. On sterile dung, M2 minimal medium and M0 medium supplemented with wood shavings as carbon sources (a medium with an heterogeneity similar to that of *P. anserina* natural substrate, but with a composition better controlled), heterokaryons were stable as the culture retained both mating types, as seen by the ability of the cultures to differentiate fertilized fruiting bodies, up to senescence (Figure 4).

We then assayed if *mat*+/*mat*+ or *mat*−/*mat*− heterokaryons were less stable than *mat*+/*mat*− ones. To this end, we used strains marked with either hygromycin B or phleomycin-resistance markers and used the M0 medium supplemented with wood shavings as a carbon source. We tested two independent couples of hygromycin B and phleomycin-resistant transgenes as the insertion point may affect the stability of heterokaryons. The same transgene was associated with each mating type, by genetic crosses. Phenotypic analysis of all transgenic strains, either *mat*+ or *mat*−, did not show any phenotypic differences with wild type: the homokaryotic strains grew at the same rate as wild type on M0 with wood shavings, indicating that each nuclear genotype has the same rate of division. To measure stability, hygromycin B- and phleomycin-resistant heterokaryons in all *mat* combinations (*i.e.*, *mat*+/*mat*+, *mat*−/*mat*−, *mat*+/*mat*−, and *mat*−/*mat*+) were inoculated in three replica plates containing M0 with wood shavings and lacking both antifungal compounds. Mycelia were allowed to grow for 6.5 cm, at which point five 0.5 × 0.5 × 0.5 mm explants were taken at the growing edge of the thalli. The 15 explants were then tested for their resistance to hygromycin B and phleomycin. Data are reported in Table 2. For transgenic couple 1, all explants showed resistance to both hygromycin B and phleomycin, in all *mat* combinations, while for transgenic couple 2, phleomycin resistance was lost from all explants originating from hyg^R *mat*+/$phleo^R$ *mat*− and hyg^R *mat*−/$phleo^R$ *mat*− heterokaryon plates. This showed (1) that *mat*+/*mat*+ and *mat*−/*mat*− heterokaryons appear as stable as *mat*+/*mat*− ones, at least in the conditions investigated here, and (2) that one of the phleomycin-resistant transgene promoted a disadvantage in heterokaryon only when associated with the *mat*− mating type, although we could not detect any noticeable phenotypic difference in all used homokaryotic strains.

Discussion

Like many eukaryotic organisms, heterothallic fungi need to find a suitable partner to engage sexual reproduction. Given the numerous sexual lifestyles found in fungi, solutions to this problem are very diverse in these organisms (Billiard *et al.* 2012). Like homothallism, pseudohomothallism, a sexual lifestyle chosen by several fungi, enables both outcrossing and inbreeding. However, unlike homothallic species, pseudohomothallic species are faced with the problem of regulating heterokaryosis. In the basidiomycetes, the problem of maintaining heterokaryons is solved by the presence of a dedicated cellular structure, since dikaryons are a normal part of the life cycle in most species of *Basidiomycota* and, following plasmogamy, dikaryosis is faithfully maintained by clamp connections. In pseudohomothallic ascomycetes, whether selfing-competent dikaryons are maintained or counterselected by a dedicated mechanism is unknown. To better understand this important feature of the fungal life cycle, we have first characterized the *mat* region of *P. anserina*, *i.e.*, the chromosomic region encompassing the mating-type idiomorphs and in which recombination is severely inhibited. We found it to be a ≈800-kb region, containing > 200 genes, yet with little coding differences and lacking rearrangements between the two mating-partner nuclei.

Inhibition of recombination around the sex-determining mating type is a common phenomenon in fungi (Heitman *et al.* 2013). It has been well documented for two pseudohomothallic ascomycetes, *N. tetrasperma* and *P. anserina*, and for the heterothallic basidiomycetes *Cryptococcus spp.* and *Microbotrym lychnidis-dioicae* (Marcou *et al.* 1979; Merino

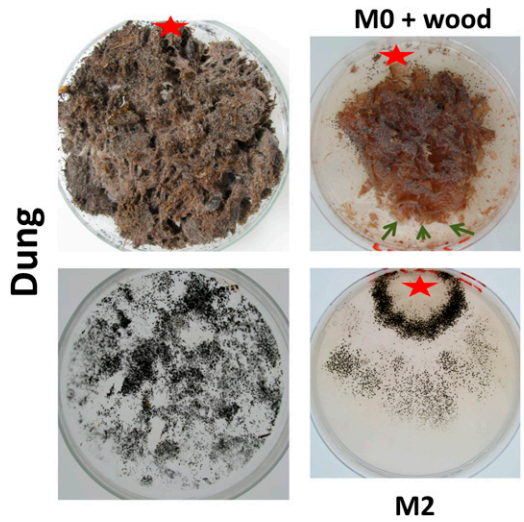

Figure 4 Stability of S *mat*+/*mat*− heterokaryons. S *mat*+/S *mat*− heterokaryons were inoculated at the positions indicated by the red stars and the plates were incubated for 10 days before the pictures were taken. Fruiting bodies appear as small black dots (green arrows on the M0 + wood shavings plate) all over the plates. As perithecia are not readily visible on dung, the cover of the plates where ascospores have been expelled is shown, indicative that perithecia are present all over dung. On M0 + wood shavings, perithecia are differentiated only on the shavings. On M2, perithecia are mostly differentiated in a 1-cm-thick ring located 1 cm away from the inoculation, but additional perithecia are differentiated further away. Only at the end of the plate perithecia are missing. However, at this location senescence has occurred, preventing fruiting.

et al. 1996; Gallegos *et al.* 2000; Fraser *et al.* 2004; Jacobson 2005; Hsueh *et al.* 2006; Metin *et al.* 2010; Ellison *et al.* 2011; Hood *et al.* 2013). In *N. tetrasperma*, complete sequencing of the genomes of *mat A* and *mat a* strains has revealed several inversions on a ≈7.8-Mb region of the ≈9.4-Mb chromosome 1 carrying the mating type (Ellison *et al.* 2011). In *Cryptococcus ssp*., different genes are present in the mating-type regions, which are ≈100 kb large, preventing meiotic pairing (Fraser *et al.* 2004; Hsueh *et al.* 2006; Metin *et al.* 2010). In *M. lychnidis-dioicae*, optical mapping has shown extensive divergence over 90% of the sex chromosomes (Hood *et al.* 2013). In all these fungi, improper pairing can thus account for the lack of recombination. The data reported here indicate that the mechanism for recombination inhibition is likely to be very different in *P. anserina*. The *mat* region devoid of recombination is only ≈0.8 Mb of the ≈8.8-Mb chromosome 1 that carries the mating type. Regions from both mating types are perfectly colinear in both S *mat*+ and S *mat*−, except at the mating-type idiomorphs, which call for a recombination inhibition that does not rely on inversion complexes or sequence divergence. This is in line with previous studies showing that, although severely repressed, recombination can occur in the *mat* region in *P. anserina* (Contamine *et al.* 1996). Such a low level of recombination could be sufficient to maintain the colinearity of both *mat* regions. In *C. neoformans*, meiotic recombination hotspots flank the unpaired region (Hsueh *et al.* 2006) and conversion occurs within the mat locus (Sun *et al.* 2012), showing that patterns of recombination in this fungus may be more complex than expected. A similar phenomenon may occur in *P. anserina*, as we identified two potential converted regions of 15 kb.

A candidate *cis*-element for shaping the recombination pattern of the *mat* region is CLR as it bears some resemblance to a centromere with its accumulation of transposons mutated by RIP. Data from several organisms show that crossing-over is inhibited around centromeres by as-yet unclear mechanism(s) possibly involving repeat-promoted heterochromatin and/or centromere-specific epigenetic marks (Talbert and Henikoff 2010). Deletion of CLR did not result in increased recombination in the *mat* region, even after five generations that should have enabled the removal of an epigenetic mark. Although we cannot rule out a mark stable enough to pass through several rounds of meiosis, we speculate that, like for centromere, another *cis*-acting element may be involved (Talbert and Henikoff 2010). Unfortunately, close inspection of the *mat* region does not reveal any obvious candidate. We speculate that structuration by such elements results in a special kind of chromatin domain over the *mat* region endowed with normal transcriptional activity, *i.e.*, not akin to heterochromatin. Indeed, several highly transcribed genes, such as *AS4* encoding translation elongation factor eEF1A and *su12* encoding a ribosomal protein, are present within the *mat* region. Another possibility is that this element structures heterochromatin specifically during meiosis or even only prophase 1 of meiosis, allowing expression of the *mat* region during the other stages of the life cycle.

The *N. tetrasperma* genome sequences uncovered 190,728 nucleotide differences between the 7.8-Mb nonrecombining regions (Ellison *et al.* 2011) resulting in degeneration in codon usage for both *mat A* and *mat a* (Whittle *et al.* 2011). This amounts to one difference on average every 40 nucleotides, a rate 30 times higher than the differences observed between the *P. anserina mat* regions and that extends in a stretch of DNA 10 times larger. Two hypotheses may account for the limited differences between the *mat* regions in *P. anserina*. First, they may have a more recent origin. However, sequencing the genome of strain T showed that strain T genome has an average 1–2% divergence with strain S genome (P. Silar, unpublished data), a value 10 times higher than the differences in the *mat* region of strain S. Yet, this strain, like all the known strains of *P. anserina* and its sibling species *Podospora comata*, is also pseudohomothallic. It can be crossed with strain S and the progeny of such mating are also pseudohomothallic and have normal mating ability. Therefore, pseudohomothallism appears to be an ancestral condition in *P. anserina* and *P. comata*, arguing against a recent origin of the mating-type region. Alternatively, conversions may homogenize the *mat* region. The fact that the sequences directly bordering the mating type contain a high number of polymorphisms and the presence of several large regions devoid of polymorphisms that

Table 2 Stability of *mat+/mat−* *vs.* *mat+/mat+* and *mat−/mat−* heterokaryons

Transgene couple	Hyg *mat* + /phleo *mat+*	Hyg *mat−*/phleo *mat−*	Hyg *mat−*/phleo *mat+*	Hyg *mat+*/phleo *mat−*
1	15 H^R P^R	15 H^R P^R	15 H^R P^R	15 H^R P^R
2	15 H^R P^R	15 H^R P^S	15 H^R P^R	15 H^R P^S

could be traces of conversion support this hypothesis. Moreover, conversion has been detected in the *mat* region (Contamine *et al.* 1996) and has also been evidenced in the mating-type region of *N. tetrasperma* (Menkis *et al.* 2010). If recombination inhibition proceeds as in centromeres, conversion may nonetheless occur, because it has been observed in centromeres (Talbert and Henikoff 2010).

Regarding the differences in coding capacity, a few polymorphic genes are present in the *mat* region in addition to the previously characterized mating idiomorphs (Picard *et al.* 1991; Debuchy and Coppin 1992) and the *rmp1* gene (Contamine *et al.* 2004), although nonsilent polymorphisms are strongly counterselected. The role(s) of the polymorphisms in most of these genes is presently unknown, but none seems involved in the definition of the mating identity, which relies exclusively on the *mat* idiomorphs (Coppin *et al.* 1993). Moreover, our microarray analysis uncovered dissimilarities in transcript accumulation of 1054 genes. This gene number is much higher than the 196 genes that exhibited a mating-type biased expression in *N. tetrasperma* (Samils *et al.* 2013). As proposed by the authors, it is possible that they underestimated the differences between *N. tetrasperma* mating types because they used microarrays designed for *N. crassa*. *N. tetrasperma* displayed an excess of *mat A* (*MAT1-1* in the standard nomenclature; Turgeon and Yoder 2000) upregulated genes on crossing medium (Samils *et al.* 2013). This feature is conserved in *P. anserina*, which also displayed a large excess of genes highly expressed in *mat−* (*MAT1-1* in the standard nomenclature) in crossing conditions (683 highly expressed genes in *mat−*, 371 highly expressed genes in *mat+*). However, there is no evidence in *P. anserina* to support the idea that sex-specific selection resulted in the feminization of the *mat−* chromosome and masculinization of the *mat+* chromosome, as proposed in *N. tetrasperma*. In fact, the conclusion in *N. tetrasperma* was based on quantitative analyses of microarray, while any valid conclusion in this matter will require functional analyses of the genes differentially expressed in strains of opposite mating types. Moreover, the phenotype of homokaryotic *N. tetrasperma* strains seems to contradict the proposal of Samils *et al.* (2013), as the *mat A* strain, which was proposed to contain a feminized *mat* region, produces in fact fewer protoperithecia (Howe 1964) than the supposedly masculinized *mat a* strain. Size differences were also reported for protoperithecia in *mat a* and *mat A* strains (Howe 1964). This observation suggests that some metabolic differences may be related to quality differences in protoperithecial production. It is likely that protoperithecial quality differences correlate with ascospore production per perithecium, which could be a more pertinent indicator of feminization than protoperithecium number. Further analyses will be required to determine whether ascospore number per perithecium is different in *mat a* and *mat A* strain.

Analysis of the linkage group distribution of the 1054 genes showed no overrepresentation of genes, especially in the *mat* region, whereas the recombination-suppressed regions of *N. tetrasperma* are enriched in highly expressed genes. Samils *et al.* (2013) observed that the mating-type bias in gene expression accumulates as a consequence of sequence divergence. It is likely that the number of polymorphisms is too small in the *P. anserina mat* region to induce a bias in the number of differentially expressed genes on chromosome 1. The 194 investigated genes regulated specifically by the *mat* region and the 46 genes with the highest differences are mostly genes coding enzymes from various metabolisms, suggesting that S *mat+* and S *mat−* present metabolic differences. While the triggering of premature death and thermosensitivity are controlled by *rmp1*, previous data suggest that *rmp1* does not control the life span difference between S *mat+* and S *mat−* (Contamine *et al.* 1996). Longevity in *P. anserina* appears to be strongly connected to metabolism (Rossignol and Silar 1996; Silar *et al.* 2001), especially respiration (Dufour *et al.* 2000). The potential metabolic differences evidenced here, especially the differences in the level of the mitochondria-encoded *nad1*, *nad2*, and *nad3* transcripts, may thus account for the different life span of the S *mat+* and S *mat−* strains. The last detected difference between S *mat+* and S *mat−* is in the efficiency of the *su8-1* suppression (Silar *et al.* 2000). The *su8-1* suppressor tRNA acts by pairing with UGA stop codon and allowing translational readthrough (Debuchy and Brygoo 1985). In the list of *mat+/mat−* polymorphic genes (Table S2), there is no obvious candidate gene whose product would interact with tRNAs or the translation machinery. Action on translation could result from an indirect effect. For example, the S *mat+* *vs.* S *mat−* differentially regulated *Pa_7_9690*, participating in the post-translational modification of proteins, may be involved and could act on a factor that directly interacts with *su8-1*, such as eEF1A or the ribosome. Alternatively, differences in the expression of ribosomal proteins may be involved since Rp115, Rp127, Rp1P0, and Rp17 are differentially regulated in S *mat+* and S *mat−* (Table S3). It is currently not possible to determine whether all these differences between *mat+* and *mat−* strains are random, or selected to promote complementation between S *mat+* and S *mat−* nuclei (*i.e.*, inbreeding) or heterokaryons breakthrough (*i.e.*, outcrossing).

Inoculation of *P. anserina* on its natural substrate or on artificial substrates shows that heterokaryotic mycelia retain both *mat+* and *mat−* nuclei. This suggests that in nature *P. anserina mat+/mat−* heterokaryotic mycelia are very stable and that *P. anserina*, or at least the strains that behave like S, are unlikely to lose one of the mating types by mitotic segregation during growth on its restricted biotope. It thus appears that this species prefers inbreeding to outcrossing. However, we cannot rule out that under natural conditions, when other fungi compete for dung exploitation or when environmental conditions are more variable, heterokaryosis is lost more frequently than anticipated from our controlled lab experiments. Indeed, although we did not detect differences between heterokaryotic and homokaryotic strains in our controlled experiments, we know that at 37° S *mat+* and S *mat−* behave clearly differently (Contamine *et al.* 2004), arguing that under more stressful conditions, having both *mat+* and *mat−* nuclei may be advantageous. Data regarding the choice of inbreeding or outcrossing in *N. tetrasperma* are inconclusive. On one hand, homokaryotic conidia may frequently be recovered (Metin *et al.* 2010; Corcoran *et al.* 2012), and on the other, outcrossing is associated with sexual dysfunctions (Jacobson 1995). In both species, the versatility of pseudohomothallism may be advantageous in selecting for inbreeding as the preferred mode of reproduction, yet sometimes forcing outcrossing when heterokaryons break down.

A surprising result from this study is the fact that despite physiological differences in the S *mat+* and S *mat−* strains, this does not seem to affect the stability of heterokaryons in either way: more or less stability. Indeed, we found that *P. anserina* undergoes senescence before losing nuclei in the absence of selective pressure. That genetic factors may control heterokaryon stability in *P. anserina* is demonstrated by transgene couple 2 (Table 2). While we did not detect any obvious difference in growth of all homokaryotic strains for all transgenic strains, the *phleo^R mat−* nuclei of couple 2 are systematically lost when associated with either the *hyg^R mat+* or *hyg^R mat−* nuclei, while the *phleo^R mat+* nuclei are retained. Yet, in both cases, the resistance to phleomycin is promoted by the same transgene. This does not happen with couple 1, although the same plasmid was used to create the phleomycin-resistant strain, showing that this effect is actually due to the insertion of the transgene in couple 2.

Intriguingly, in *A. bisporus*, a pseudohomothallic basidiomycete, clamp connections are missing and hyphae are multinucleated. Like in the case of *P. anserina*, it is not clear how heterokaryosis could be maintained in this fungus (Raper *et al.* 1972; Raper and Kaye 1978). A first candidate is anastomosis. However, leading hyphae growing at the edge of the colony, which are those most likely to generate homokaryotic sectors by loss of one of the two kinds of nuclei, do not undergo anastomosis (Buller 1933). A second possibility could be the nuclear mixing recently discovered in *N. crassa* (Roper *et al.* 2013). This mechanism is not involved in the maintenance of sexually compatible nuclei, but likely enables mycelium fitness in variable environments. In this instance, stability of heterokaryons in *P. anserina* may not have required the selection of a special mechanism to maintain sexual heterokaryosis. Nuclear mixing can indeed explain the stability of *mat+/mat−* heterokaryons in *P. anserina*. It may be a general phenomenon in fungi and may also account for the stability of heterokaryons in *A. bisporus*, but also in *Heterobasidion parvisporum*, in which nuclear ratios are imbalanced, genetically determined, and stable over time (James *et al.* 2008).

Acknowledgments

We thank Sylvie François for expert technical assistance and Ibtissen Grissa who participated in the early stages of this work. P.G. is a recipient of a "nouveau contrat doctoral" fellowship from Université Paris Diderot, Paris 7, Sorbonne Paris cité.

Literature Cited

Ausubel, F. M., R. Brent, R. E. Kingston, D. D. Moore, J. G. Seidman *et al.* (Editors), 1987 *Current Protocoles in Molecular Biology.* Wiley Interscience, New York.

Belcour, L., O. Begel, and M. Picard, 1991 A site-specific deletion in mitochondrial DNA of *Podospora* is under the control of nuclear genes. Proc. Natl. Acad. Sci. USA 88: 3579–3583.

Benjamini, Y., and Y. Hochberg, 1995 Controlling the false discovery rate: a practical and powerful approach to multiple testing. J. R. Stat. Soc. B 57: 289–300.

Bidard, F., S. Imbeaud, N. Reymond, O. Lespinet, P. Silar *et al.*, 2010 A general framework for optimization of probes for gene expression microarray and its application to the fungus *Podospora anserina*. BMC Res. Notes 3: 171.

Bidard, F., J. Ait Benkhali, E. Coppin, S. Imbeaud, P. Grognet *et al.*, 2011 Genome-wide gene expression profiling of fertilization competent mycelium in opposite mating types in the heterothallic fungus *Podospora anserina*. PLoS ONE 6: e21476.

Bidard, F., E. Coppin, and P. Silar, 2012 The transcriptional response to the inactivation of the PaMpk1 and PaMpk2 MAP kinase pathways in *Podospora anserina*. Fungal Genet. Biol. 49: 643–652.

Billiard, S., M. Lopez-Villavicencio, M. E. Hood, and T. Giraud, 2012 Sex, outcrossing and mating types: unsolved questions in fungi and beyond. J. Evol. Biol. 25: 1020–1038.

Bonnet, C., E. Espagne, D. Zickler, S. Boisnard, A. Bourdais *et al.*, 2006 The peroxisomal import proteins PEX2, PEX5 and PEX7 are differently involved in *Podospora anserina* sexual cycle. Mol. Microbiol. 62: 157–169.

Buller, A. H. R., 1933 The formation of hyphal fusions in the mycelium of the higher fungi, pp. 1–74 in *Researches on Fungi*. Longmans Green & Co., London.

Cheeseman, K., J. Ropars, P. Renault, J. Dupont, J. Gouzy *et al.*, 2014 Multiple recent horizontal transfers of a large genomic region in cheese making fungi. Nat Commun 5: 2876.

Contamine, V., G. Lecellier, L. Belcour, and M. Picard, 1996 Premature death in *Podospora anserina*: sporadic accumulation of the deleted mitochondrial genome, translational parameters and innocuity of the mating types. Genetics 144: 541–555.

Contamine, V., D. Zickler, and M. Picard, 2004 The *Podospora rmp1* gene implicated in nucleus-mitochondria cross-talk encodes an essential protein whose subcellular location is developmentally regulated. Genetics 166: 135–150.

Coppin, E., S. Arnaise, V. Contamine, and M. Picard, 1993 Deletion of the mating type sequences in *Podospora anserina* abolishes mating without affecting vegetative functions and sexual differentiation. Mol. Gen. Genet. 241: 409–414.

Corcoran, P., D. J. Jacobson, M. I. Bidartondo, P. C. Hickey, J. F. Kerekes *et al.*, 2012 Quantifying functional heterothallism in the pseudohomothallic ascomycete *Neurospora tetrasperma*. Fungal Biol 116: 962–975.

Debuchy, R., and Y. Brygoo, 1985 Cloning of opal suppressor tRNA genes of a filamentous fungus reveals two tRNASerUGA genes with unexpected structural differences. EMBO J. 4: 3553–3556.

Debuchy, R., and E. Coppin, 1992 The mating types of *Podospora anserina*: functional analysis and sequence of the fertilization domains. Mol. Gen. Genet. 233: 113–121.

Dodge, B. O., 1932 Crossing hermaphroditic races of *Neurospora*. Mycologia 24: 7–13.

Dowding, E. S., 1931 The sexuality of the normal, giant and dwarf spores of *Pleurage anserina*. (Ces). Kuntze. Ann. Bot. 45: 1–14.

Dranginis, A. M., J. M. Rauceo, J. E. Coronado, and P. N. Lipke, 2007 A biochemical guide to yeast adhesins: glycoproteins for social and antisocial occasions. Microbiol. Mol. Biol. Rev. 71: 282–294.

Dufour, E., J. Boulay, V. Rincheval, and A. Sainsard-Chanet, 2000 A causal link between respiration and senescence in *Podospora anserina*. Proc. Natl. Acad. Sci. USA 97: 4138–4143.

El-Khoury, R., C. H. Sellem, E. Coppin, A. Boivin, M. F. Maas *et al.*, 2008 Gene deletion and allelic replacement in the filamentous fungus *Podospora anserina*. Curr. Genet. 53: 249–258.

Ellison, C. E., J. E. Stajich, D. J. Jacobson, D. O. Natvig, A. Lapidus *et al.*, 2011 Massive changes in genome architecture accompany the transition to self-fertility in the filamentous fungus *Neurospora tetrasperma*. Genetics 189: 55–69.

Espagne, E., O. Lespinet, F. Malagnac, C. Da Silva, O. Jaillon *et al.*, 2008 The genome sequence of the model ascomycete fungus *Podospora anserina*. Genome Biol. 9: R77.

Fraser, J. A., S. Diezmann, R. L. Subaran, A. Allen, K. B. Lengeler *et al.*, 2004 Convergent evolution of chromosomal sex-determining regions in the animal and fungal kingdoms. PLoS Biol. 2: e384.

Galagan, J. E., and E. U. Selker, 2004 RIP: the evolutionary cost of genome defense. Trends Genet. 20: 417–423.

Gallegos, A., D. J. Jacobson, N. B. Raju, M. P. Skupski, and D. O. Natvig, 2000 Suppressed recombination and a pairing anomaly on the mating type chromosome of *Neurospora tetrasperma*. Genetics 154: 623–633.

Graïa, F., V. Berteaux-Lecellier, D. Zickler, and M. Picard, 2000 *ami1*, an orthologue of the *Aspergillus nidulans apsA* gene, is involved in nuclear migration events throughout the life cycle of *Podospora anserina*. Genetics 155: 633–646.

Grognet, P., H. Lalucque, and P. Silar, 2012 The PaAlr1 magnesium transporter is required for ascospore development in *Podospora anserina*. Fungal Biol. 116: 1111–1118.

Heitman, J., S. Sun, and T. Y. James, 2013 Evolution of fungal sexual reproduction. Mycologia 105: 1–27.

Hood, M. E., E. Petit, and T. Giraud, 2013 Extensive divergence between mating type chromosomes of the anther-smut fungus. Genetics 193: 309–315.

Horton, P., K. J. Park, T. Obayashi, N. Fujita, H. Harada *et al.*, 2007 WoLF PSORT: protein localization predictor. Nucleic Acids Res. 35: W585–W587.

Howe, H. B. Jr., 1964 Vegetative traits associated with mating type in *Neurospora tetrasperma*. Mycologia 56: 519–525.

Hsueh, Y.-P., A. Idnurm, and J. Heitman, 2006 Recombination hotspots flank the *Cryptococcus* mating type locus: implications for the evolution of a fungal sex chromosome. PLoS Genet. 2: e184.

Imbeaud, S., E. Graudens, V. Boulanger, X. Barlet, P. Zaborski *et al.*, 2005 Towards standardization of RNA quality assessment using user-independent classifiers of microcapillary electrophoresis traces. Nucleic Acids Res. 33: e56.

Jacobson, D. J., 1995 Sexual dysfunction associated with outcrossing in *Neurospora tetrasperma*, a pseudohomothallic ascomycete. Mycologia 87: 604–617.

Jacobson, D. J., 2005 Blocked recombination along the mating type chromosomes of *Neurospora tetrasperma* involves both structural heterozygosity and autosomal genes. Genetics 171: 839–843.

James, T. Y., J. Stenlid, A. Olson, and H. Johannesson, 2008 Evolutionary significance of imbalanced nuclear ratios within heterokaryons of the basidiomycete fungus *Heterobasidion parviporum*. Evolution 62: 2279–2296.

Lambou, K., F. Malagnac, C. Barbisan, D. Tharreau, M. H. Lebrun *et al.*, 2008 The crucial role during ascospore germination of the Pls1 tetraspanin in *Podospora anserina* provides an example of the convergent evolution of morphogenetic processes in fungal plant pathogens and saprobes. Eukaryot. Cell 7: 1809–1818.

Li, H., B. Handsaker, A. Wysoker, T. Fennell, J. Ruan *et al.*, 2009 The sequence alignment/map format and SAMtools. Bioinformatics 25: 2078–2079.

Marcou, D., 1961 Notion de longévité et nature cytoplasmique du déterminant de la sénescence chez quelques champignons. Ann. Sci. Natur. Bot. Paris Sér. 12 2: 653–764.

Marcou, D., A. Masson, J. M. Simonet, and G. Piquepaille, 1979 Evidence for non-random spatial distribution of meiotic exchanges in *Podospora anserina*: comparison between linkage groups 1 and 6. Mol. Gen. Genet. 176: 67–79.

Marisa, L., J. L. Ichante, N. Reymond, L. Aggerbeck, H. Delacroix *et al.*, 2007 MAnGO: an interactive R-based tool for two-colour microarray analysis. Bioinformatics 23: 2339–2341.

Martin, E. M., 1940 The morphology and cytology of *Taphrina deformans*. Am. J. Bot. 27: 743–751.

Menkis, A., C. A. Whittle, and H. Johannesson, 2010 Gene genealogies indicates abundant gene conversions and independent evolutionary histories of the mating type chromosomes in the evolutionary history of *Neurospora tetrasperma*. BMC Evol. Biol. 10: 234.

Merino, S. T., M. A. Nelson, D. J. Jacobson, and D. O. Natvig, 1996 Pseudohomothallism and evolution of the mating type chromosome in *Neurospora tetrasperma*. Genetics 143: 789–799.

Metin, B., K. Findley, and J. Heitman, 2010 The mating type locus (MAT) and sexual reproduction of *Cryptococcus heveanensis*: insights into the evolution of sex and sex-determining chromosomal regions in fungi. PLoS Genet. 6: e1000961.

Nakamura, T., A. Ando, H. Takagi, and J. Shima, 2007 EOS1, whose deletion confers sensitivity to oxidative stress, is involved in *N*-glycosylation in *Saccharomyces cerevisiae*. Biochem. Biophys. Res. Commun. 353: 293–298.

Picard, M., R. Debuchy, and E. Coppin, 1991 Cloning the mating types of the heterothallic fungus *Podospora anserina*: developmental features of haploid transformants carrying both mating types. Genetics 128: 539–547.

Raju, N. B., 1992 Functional heterothallism resulting from homokaryotic conidia and ascospores in *Neurospora tetrasperma*. Mycol. Res. 96: 103–116.

Raju, N. B., and D. D. Perkins, 1994 Diverse programs of ascus development in pseudohomothallic species of *Neurospora*, *Gelasinospora*, and *Podospora*. Dev. Genet. 15: 104–118.

Raper, C. A., and G. Kaye, 1978 Sexual and other relationships in the genus *Agaricus*. J. Gen. Mic. 105: 135–151.

Raper, C. A., J. R. Raper, and R. E. Miller, 1972 Genetic analysis of the life cycle of *Agaricus bisporus*. Mycologia 64: 1088–1117.

Rizet, G., and G. Delannoy, 1950 Sur la production par des hétérozygotes monofactoriels de *Podospora anserina* de gaméto-

phytes phénotypiquement différents des gamétophytes parentaux. C. R. Acad. Sci. Paris 231: 588–590.

Rizet, G., and C. Engelmann, 1949 Contribution à l'étude génétique d'un Ascomycète tétrasporé: *Podospora anserina* (Ces.). Rehm. Rev. Cytol. Biol. Veg. 11: 201–304.

Roper, M., A. Simonin, P. C. Hickey, A. Leeder, and N. L. Glass, 2013 Nuclear dynamics in a fungal chimera. Proc. Natl. Acad. Sci. USA 110: 12875–12880.

Rossignol, M., and P. Silar, 1996 Genes that control longevity in *Podospora anserina*. Mech. Ageing Dev. 90: 183–193.

Samils, N., A. Gioti, M. Karlsson, Y. Sun, T. Kasuga *et al.*, 2013 Sex-linked transcriptional divergence in the hermaphrodite fungus *Neurospora tetrasperma*. Proc. Biol. Sci. 280: 20130862.

Silar, P., 1995 Two new easy-to-use vectors for transformations. Fungal Genet. Newsl. 42: 73.

Silar, P., 2011 Grafting as a method for studying development in the filamentous fungus *Podospora anserina*. Fungal Biol 115: 793–802.

Silar, P., 2013 *Podospora anserina*: from laboratory to biotechnology, pp. 283–309 in *Genomics of Soil- and Plant-Associated Fungi*, edited by P. K. M. Benjamin, A. Horwitz, M. Mukherjee, and C. P. Kubicek, Springer, Heidelberg/New York/Dordrecht/London.

Silar, P., and M. Picard, 1994 Increased longevity of EF-1 alpha high-fidelity mutants in *Podospora anserina*. J. Mol. Biol. 235: 231–236.

Silar, P., F. Koll, and M. Rossignol, 1997 Cytosolic ribosomal mutations that abolish accumulation of circular intron in the mitochondria without preventing senescence of *Podospora anserina*. Genetics 145: 697–705.

Silar, P., M. Rossignol, V. Haedens, Z. Derhy, and A. Mazabraud, 2000 Deletion and dosage modulation of the *eEF1A* gene in *Podospora anserina*: effect on the life cycle. Biogerontology 1: 47–54.

Silar, P., H. Lalucque, and C. Vierny, 2001 Cell degeneration in the model system *Podospora anserina*. Biogerontology 2: 1–17.

Soid-Raggi, G., O. Sanchez, and J. Aguirre, 2006 TmpA, a member of a novel family of putative membrane flavoproteins, regulates asexual development in *Aspergillus nidulans*. Mol. Microbiol. 59: 854–869.

Sun, S., Y. P. Hsueh, and J. Heitman, 2012 Gene conversion occurs within the mating type locus of *Cryptococcus neoformans* during sexual reproduction. PLoS Genet. 8: e1002810.

Talbert, P. B., and S. Henikoff, 2010 Centromeres convert but don't cross. PLoS Biol. 8: e1000326.

Turgeon, B. G., and R. Debuchy, 2007 *Cochliobolus and Podospora: Mechanisms of Sex Determination and the Evolution of Reproductive Lifestyle in Sex in Fungi: Molecular Determination and Evolutionary Implications*, edited by J. Heitman, J. W. Kronstad, J. W. Taylor and L. A. Casselton ASM Press, Washington, DC.

Turgeon, B. G., and O. C. Yoder, 2000 Proposed nomenclature for mating type genes of filamentous ascomycetes. Fungal Genet. Biol. 31: 1–5.

Whittle, C. A., Y. Sun, and H. Johannesson, 2011 Degeneration in codon usage within the region of suppressed recombination in the mating type chromosomes of *Neurospora tetrasperma*. Eukaryot. Cell 10: 594–603.

Zerbino, D. R., and E. Birney, 2008 Velvet: algorithms for *de novo* short read assembly using de Bruijn graphs. Genome Res. 18: 821–829.

Communicating editor: E. U. Selker

GENETICS

Supporting Information
http://www.genetics.org/lookup/suppl/doi:10.1534/genetics.113.159988/-/DC1

Maintaining Two Mating Types: Structure of the Mating Type Locus and Its Role in Heterokaryosis in *Podospora anserina*

Pierre Grognet, Frédérique Bidard, Claire Kuchly, Laetitia Chan Ho Tong, Evelyne Coppin, Jinane Ait Benkhali, Arnaud Couloux, Patrick Wincker, Robert Debuchy, and Philippe Silar

DOI: 10.1534/genetics.113.159988

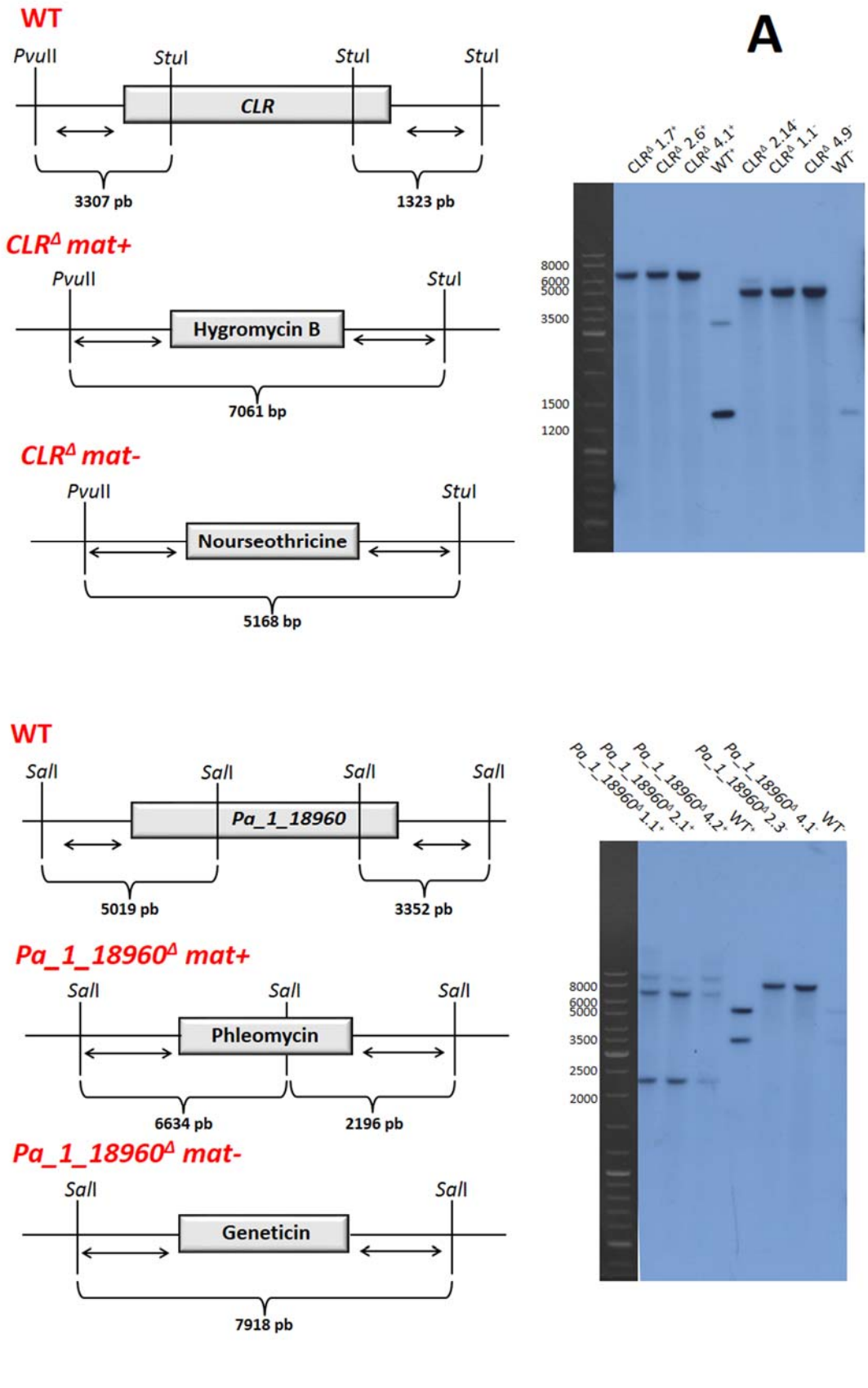
WT
PvuII
StuI
StuI
StuI
CLR
3307 pb
1323 pb
CLRΔ mat+
PvuII
StuI
Hygromycin B
7061 bp
CLRΔ mat-
PvuII
StuI
Nourseothricine
5168 bp
A
CLRΔ 1.7+
CLRΔ 2.6+
CLRΔ 4.1+
WT+
CLRΔ 2.14-
CLRΔ 1.1-
CLRΔ 4.9-
WT-
8000
6000
5000
3500
1500
1200
WT
SalI
SalI
SalI
SalI
Pa_1_18960
5019 pb
3352 pb
Pa_1_18960Δ mat+
SalI
SalI
SalI
Phleomycin
6634 pb
2196 pb
Pa_1_18960Δ mat-
SalI
SalI
Geneticin
7918 pb
Pa_1_18960Δ 1.1+
Pa_1_18960Δ 2.1+
Pa_1_18960Δ 4.2+
WT+
Pa_1_18960Δ 2.3-
Pa_1_18960Δ 4.1-
WT-
8000
6000
5000
3500
2500
2000

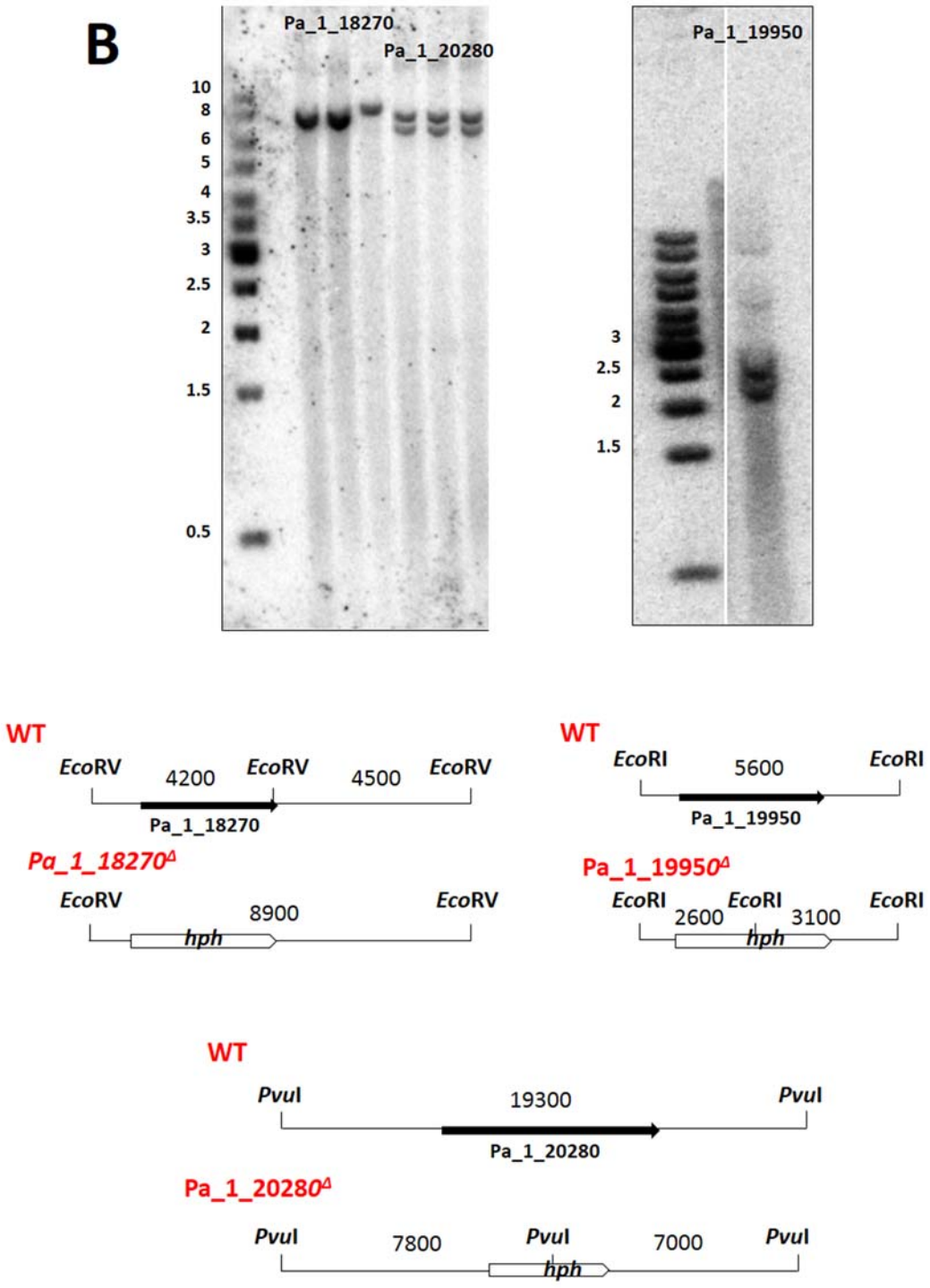

Figure S1 (A) Southern blot validation of CLR and *Pa_1_18960* replacements. Left: schematic representation of wild type (WT) and replaced DNA regions. The probes used are a mix of the DNA regions indicated as double arrows, as to probe for regions the upstream and downstream of the replacement. DNA was digested with the indicated enzymes. **(B) Genomic Southern blots of candidate agglutinin mutant strains.** DNA from one or several candidate transformants was digested with the indicated relevant enzyme and probed with the hygromycin B resistance gene. All tested transformants displayed the expected pattern for homologous recombination.

```
Mat+: 1    MRNRTGQAILAVLLTILSFAGITDGQAYYGTVQRELQACGSDNFINLGCFKNFISVAQPT
Mat-: 1    MRNRTGQAILAVLLTILSFAGITDGQAYYGTVQRELQACGSDNFINLGCFKNFISVAQPT

Mat+: 61   YFQFDPQGYLPSDPSRSFPGWSPGSNYNNTATGLDCARACRGFGYKFAAMRDNSCRCGIQ
Mat-: 61   YFQFDPQGYLPSDPSRSFPGWSPGSNYNNTATGLDCARACRGFGYKFAAMRDNSCRCGIQ

Mat+: 121  LPVGYSPTQDAVCQIPCQGNPNQTCGGGSDAQIYVDPSFAANSQVPIQAQNPYIAGFYNY
Mat-: 121  LPVGYSPTQDAVCQIPCQGNPNQTCGGGSDAQIYVDPSFAANSQVPIQAQNPYIAGFYNY

Mat+: 181  LGCFYLPSGMPSGDSRATFTVPTVDECWNRCAGLGYPLVAGVVDSGSTRCFCGTTFGFPS
Mat-: 181  LGCFYLPSGMPSGDSRATFTVPTVDECWNRCAGLGYPLVAGVVDSGSTRCFCGTTFGFPS

Mat+: 241  FRARPELLPVPGDCNTTCTSLGGTNGNCDIATGRCCGRGPYMPVYINPELQGCYSPIIPG
Mat-: 241  FRARPELLPVPGDCNTTCTSLGGTNGNCDIATGRCCGRGPYMPVYINPELQGCYSPIIPG

Mat+: 301  FKATQAEPDYECFDPPPTSLLGPPKVLAQPSYPSSLIINTGPALIRPPSVSAGQRVYLING
Mat-: 301  FKATQAEPDYECFDPPPTSLLGPPKVLAQPSYPSSLIINTGPALIRPPSVSAGQRVYLING

Mat+: 361  CYGSSVFGTGGGTAVFNSALSLTRLNISPATLENCASICNAGNYDAMGMVNGRDCYCSPT
Mat-: 361  CYGSSVFGTGGGTAVFNSALSLTRLNISPATLENCASICNAGNYDAMGMVNGRDCYCSPT

Mat+: 421  VNSGLTFDNMGFCRVPCGDANNIACGAPNSPVVYAVNGGGVFSSYVSTQIVTPYPTYNCL
Mat-: 421  VNSGLTFDNMGFCRVPCGDANNIACGAPNSPVVYAVNGGGVFSSYVSTQIVTPYPTYNCL

Mat+: 481  GRATSFTTTSTTTTTSTTTSIQTSTSTTTTTTTSTSTSTSATATTTGTTTSTSTSTSTTTT
Mat-: 481  GRATSFTTTSTTTTTSTTTSIQTSTSTTTTTTTSTSTSTSATATTTGTTTSTSTSTSTTTT

Mat+: 541  TTSTTTTATSTSTSSTTTTSTSTTSTTTTGTSTTSTTTTGTSTTSTTTTGTSTSTSLTTT
Mat-: 541  TTSTTTTATSTSTSSTTTTSTSTTSTTTTGTSTTSTTTTGTSTTSTTTTGTSTSTSLTTT

Mat+: 601  SSTSTSLTTTTTTSTSTSLTTTSSTSTDLTTTTTTTTTSSSTSTSLTTTTTTTSSSTSTS
Mat-: 601  SSTSTSLTTTTTTSTSTSLTTTSSTSTDLTTTTTTTTSSSTSTSLTTTTTTTSSSTSTS

Mat+: 661  LTTTSSTSTDLTTTTTTTSSTSTDLTTTSTTSTSTSLTTTTTTTSSTSTSLTTTSTTSTS
Mat-: 661  LTTTSSTSTDLTTTTTTTSSTSTDLTTTSTTSTSTSLTTTTTTTSSTSTSLTTTSTTSTS

Mat+: 721  TSLTTTSSTSTDLTTTTTTTTSSSTSTSLTTTSTTSTSTSLTTTSSTSTDLTTATTTTTT
Mat-: 721  TSLTTTSSTSTDLTTTTTTTTSSSTSTSLTTTSTTSTSTSLTTTSSTSTDLTTATTTTTT

Mat+: 781  SSTSTSLTTTSTTSTSTSLTTTSSTATDLTTTTTTTTSSSTSTSLTTTSTTSTSTSLTTT
Mat-: 781  SSTSTSLTTTSTTSTSTSLTTTSSTATDLTTTTTTTTSSSTSTSLTTTSTTSTSTSLTTT

Mat+: 841  SSTSTDLTTTTTTSTSTSSTTTDTTTTTTSTSTSSTTTTGTETTSTTTSTTTTTTSTSTS
Mat-: 841  SSTSTDLTTTTTTSTSTSSTTTDTTTTTTSTSTSSTTTTGTETTSTTTSTTTTTTSTSTS

Mat+: 901  STTTTETETTSTTTDTTTTTTSTSTSISTTSTTTTGTSTSSTTTDTTTTTTSTSTSLSTT
Mat-: 901  STTTTETETTSTTTDTTTTTTSTSTSISTTSTTTTGTSTSSTTTDTTTTTTSTSTSLSTT

Mat+: 961  TSTSTSISTTSTTTTGTSTSSTTTETTTTSTSTSISTTSTTTTDTSTSSTTTTETSTTST
Mat-: 961  TSTSTSISTTSTTTTGTSTSSTTTETTTTSTSTSISTTSTTTTDTSTSSTTTTETSTTST

Mat+: 1021 TTTGTSTSSTTTETTTTSTSTSISTTSTTTTGTSTSSTTTETTTTSTSTSISTTSTTTTG
Mat-: 1021 TTTGTSTSSTTTETTTTSTSTSISTTSTTTTGTSTSSTTTETTTTSTSTSISTTSTTTTG

Mat+: 1081 TETSSTTTTGTSTTSTTTTGTSTSSTTTETTSTSTSISTSTTTTGTSTTSTTATETSTS
Mat-: 1081 TETSSTTTTGTSTTSTTTTGTSTSSTTTETTSTSTSISTSTTTTGTSTTSTTATETSTS

Mat+: 1141 TTSTTTTETSTSSTTTTGTSTTSTTTTSTSTSSTTTTGTSTSSTTTETTTTTTSTSTSTS
Mat-: 1141 TTSTTTT----------GTSTTSTTTTSTSTSSTTTTGTSTSSTTTETTTTTTSTSTSTS

Mat+: 1201 LTTTSSTSTSLTTTSSTSTSLTTTTTTSTSTSLTETTTSSTSTSLTTTTSTSTSLTETTT
Mat-: 1191 LTTTSSTSTSLTTTSSTSTSLTTTTTTSTSTSLTETTTSSTSTSLTTTTSTSTSLTETTT

Mat+: 1261 LSTSTSLTTTSSTSTSLTTTSSTSTSLTTTSSTSTSLTTTTTTSTST------------
Mat-: 1251 LSTSTSLTTTSSTSTSLTTTSSTSTSLTTTSSTSTSLTTTTTTSTSTSLTETTTSSTSTS

Mat+: 1308 ----------SLTETTTSSTSTSLTTTTTTSTSTSLTETTTSSTSTSLTTTSSTSTSLT
Mat-: 1311 LTTTTTTSTSTSLTETTTSSTSTSLTTTTTTSTSTSLTETTTSSTSTSLTTTSSTSTSLT

Mat+: 1357 TTSSTSTSLTTTTTTSTSTDLTTTSSTSTSLTTTSSTSTSLTTTDSTSTSLTTTSSTSTS
Mat-: 1371 TTSSTSTSLTTTTTTSTSTDLTTTSSTSTSLTTTSSTSTSLTTTDSTSTSLTTTSSTSTS

Mat+: 1417 LTTTTTTETSTTSTTSTDISTTSTTTTGTSTSSTTTETTTTTTSTSTSLTTTSSTSTSLT
Mat-: 1431 LTTTTTTETSTTSTTSTDISTTSTTTTGTSTSSTTTETTTTTTSTSTSLTTTSSTSTSLT

Mat+: 1477 TTTTSSTSTDVSTTSTTTTETSTSSTTTETTTTTTSTSISLTTTSSTSTSLTTTTTSSTS
Mat-: 1491 TTTTSSTSTDVSTTSTTTTETSTSSTTTETTTTTTSTSISLTTTSSTSTSLTTTTTSSTS

Mat+: 1537 TDISTTSTTTTGTSTSSTTTQTTTTTTATSTSSTTTTETSTTSTTTTSVSTSSSTTTETS
Mat-: 1551 TDISTTSTTTTGTSTSSTTTQTTTTTTATSTSSTTTTETSTTSTTTTSVSTSSSTTTETS

Mat+: 1597 TSSTTTTGTETTSTTTTGTSTTSTITTSTSISQTTSTSSTTTTGTETTSTTTTSTTTSTF
Mat-: 1611 TSSTTTTGTETTSTTTTGTSTTSTTTTSTSISQTTSTSSTTTTGTETTSTTTTSTTTSTF

Mat+: 1657 TSISETTSTSSSITTTGTSTTSTTTTSTSTSTSISETTSTSSTTTTDTSTTSTTTTSTSIS
Mat-: 1671 TSISETTSTSSSITTTGTSTTSTTTTSTSTSTSISETTSTSSTTTTDTSTTSTTTTSTSIS

Mat+: 1717 ATSTTTTGTSTTSTTTTSTSTSTSTSISQTTSTSSTTTTGTSTTSTTTTSTSTSSVTTTG
Mat-: 1731 ATSTTTTGTSTTSTTTTSTSTSTSTSISQTTSTSSTTTTGTSTTSTTTTSTSTSSVTTTG

Mat+: 1777 TETSSTTTTTTSTSTSVRETTSTSSTTTTGTSTTSTTTTSTSTSTSVSQTTSTSSTTTTG
Mat-: 1791 TETSSTTTTTTSTSTSVRETTSTSSTTTTGTSTTSTTTTSTSTSTSVSQTTSTSSTTTTG

Mat+: 1837 TSTTSTTTTTTSTSVSETTSTSSTTTTGTSTTDTTTTSTSTSTSVSETTSTSSTTTTGTS
Mat-: 1851 TSTTSTTTTTTSTSVSETTSTSSTTTTGTSTTDTTTTSTSTSTSVSETTSTSSTTTTGTS

Mat+: 1897 TTSTTTTSTSTSVSQTTSTSSTTTTGTETTSTTTTSTSTSVSETTSTSSTTTTGTSTTST
Mat-: 1911 TTSTTTTSTSTSVSQTTSTSSTTTTGTETTSTTTTSTSTSVSETTSTSSTTTTGTSTTST

Mat+: 1957 TTTSTSTSVSEITSTSSTTTTGTSTTSTTTTSTSVSQTTSTSSTTTTGTETTSTTTTSTS
Mat-: 1971 TTTSTSTSVSEITSTSSTTTTGTSTTSTTTTSTSVSQTTSTSSTTTTGTETTSTTTTSTS

Mat+: 2017 VSQTTSTSSSTTTGTSTTSTTTTTSTSTSISQTTSTSSTTTTGTSTSSTTTTGTSTTSTTT
Mat-: 2031 VSQTTSTSSTTTTGTSTTSTTTTTSTSTSISQTTSTSSTTTTGTSTSSTTTTGTSTTSTTT

Mat+: 2077 TETSTTSTTTTSTSTSVSETTSTSSTTTTGTSTTSTTTTSTSTSTSTSITQTTLTSSTTT
Mat-: 2091 TETSTTSTTTTSTSTSVSETTSTSSTTTTGTSTTSTTTTSTSTSTSTSITQTTSTSSTTT

Mat+: 2137 TGTETTSTTTTGTSTSSTTTGTSTSSTTTSTTTTGTSTTSTTTTGTSTSSTTTTDTSTT
Mat-: 2151 TGTETTSTTTTGTSTSSTTTGTGTSSTTTSTTTTGTSTTSTTTTGTSTSSTTTTDTSTT

Mat+: 2197 STTTTDTSTTSTTTTGTSTTSTTTTTGTSTSSTTTTDTSTTSTTTTGTSTTSTTSTSTSVT
Mat-: 2211 STTTTDTSTTSTTTTGTSTTSTTTTGTSTSSTTTTDTSTTSTTTTGTSTTSTTSTSTSVT

Mat+: 2257 ETISTSSTTTTGTSTTSTTTTTTSTSVNGTTSTSSTTTTGTSTTSTTTTGVSTSSTTTTG
Mat-: 2271 ETISTSSTTTTGTSTTSTTTTTTSTSVSGTTSTSSTTTTGTSTTSTTTTGVSTSSTTTTG

Mat+: 2317 TSTTSTTTTDTSSTTTTGTSTTSTTTTGTSTSSTTTTGTSTTSTTTSTTTTGTSTTSTTT
Mat-: 2331 TSTTSTTTTDTSSTTTTGTSTTSTTTTGTSTSSTTTTGTSTTSTTTSTTTTGTSTTSTTT

Mat+: 2377 TGISTTSSTTTGTSTTSTTTTDTFTTETTETSTTLTTTTGTSTTSTTTSTTTTGTSTTST
Mat-: 2391 TGISTTSSTTTGTSTTSTTTTDIFTTETTETSTTLTTTTGTSTTSTTTSTTTTGTSTTST

Mat+: 2437 TTTGTLTTSTTTTGTSTTSTTTTGTSTTSTTEISTTSTATTETSTTSTTTTGTSTTSTTG
Mat-: 2451 TTTGTLTTSTTTTGTSTTSTTTTGTSTTSTTEISTTSTATTETSTTSTTTTGTSTTSTTG

Mat+: 2497 TSTTSTTTTGTSTTSTTATDTLTSSTTTTGTSTTSTTTSTTTTGTSTTSTTTTSTSTTST
Mat-: 2511 TSTTSTTTTGTSTTSTTATDTLTSSTTTTGTSTTSTTTSTTTTGTSTTSTTTTGTSTTST

Mat+: 2557 TTTGTSTTSTTTTGTSTSSTTTTGTSTTSTTTTGTSTSSTTTTGTETSSTTTTGTSTTST
Mat-: 2571 TTTGTSTTSTTTTGTSTSSTTTTGTSTTSTTTTGTSTSSTTTTGTETSSTTTTGTSTTST

Mat+: 2617 TTTGTSTSSTTTSTTTTGTSTTSTTTTGTETTSTTTSTTTTGTSTTSTTTTGTETSSTTT
Mat-: 2631 TTTGTSTSSTTTSTTTTGTSTTSTTTTGTETTSTTTSTTTTGTSTTSTTTTGTETSSTTT

Mat+: 2677 TGTSTSSTTTTGTSTTSTTTTGTSTTSTTTTGTSTSLTTTTSTGTSTTSTTTTSTTTGTS
Mat-: 2691 TGTSTSSTTTTGTSTTSTTTTGTSTTSTTTTGTSTSLTTTTSTGTSTTSTTTTSTTTGTS

Mat+: 2737 TISTTTTGTSTSSTTTTGTSTTSTTTTGTSTSSTTATSTTSTTITGTSTTSTITTGTSTS
Mat-: 2751 TTSTTTTGTSTSSTTTTGTSTTSTTTTDTST----------

Mat+: 2797 STTTTTTGTETTSTTTSGTETSSTTTTTTGTSTSSTITTGTETTSTTTTGTSTTSTTTTS
Mat-: 2782 ----------TSTTTTGTSTTSTTTTG

Mat+: 2857 TSTSQTTSTSSTTTTGTSTSSTTTTTTSTSTSVSQTTSTSSTTTTGTSTTSTTTTGTSTS
Mat-: 2799 TSTSSTTATSTTSTTTTGTSTTSTITTGTSTSSTTTTTTGTETTSTTTSG---------

Mat+: 2917 STTTTGTSTSSSTTTTTTSTSVSQTTSTSSTTTTGTSTSSTTTTTTSTSVTETTSTSSTTT
Mat-: 2821 ------------------------------------------------------------

Mat+: 2977 TGTETTSTTTTGTSTSSTTTTGTSTTSTTTTGTSTSSTTTTTTSTSVTETTSTSSTTTTG
```

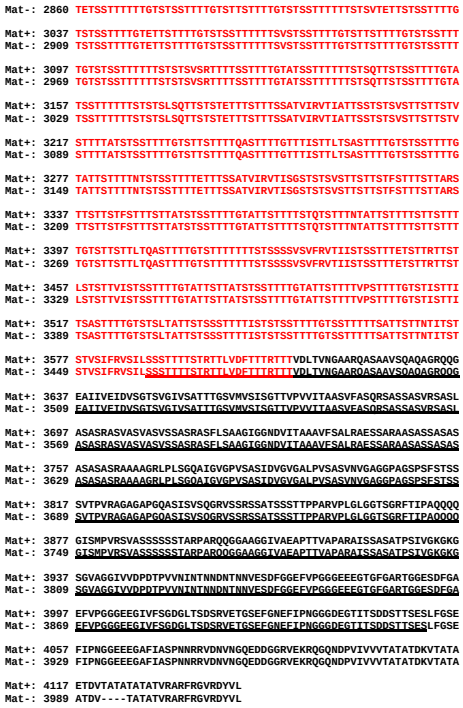

Figure S2 Comparison of *Pa_1_18960* sequence in the *mat+* and *mat-* strains. The serine/threonine-rich domain is highlighted in red. The N-terminus region similar to *NCU10264* of *N. crassa* is underlined by a thin line, the C-terminus region similar to *N. crassa NCU04373* is underlined by a thick line. The signal peptide is highlighted in orange and the three carbohydrate binding domains in green.

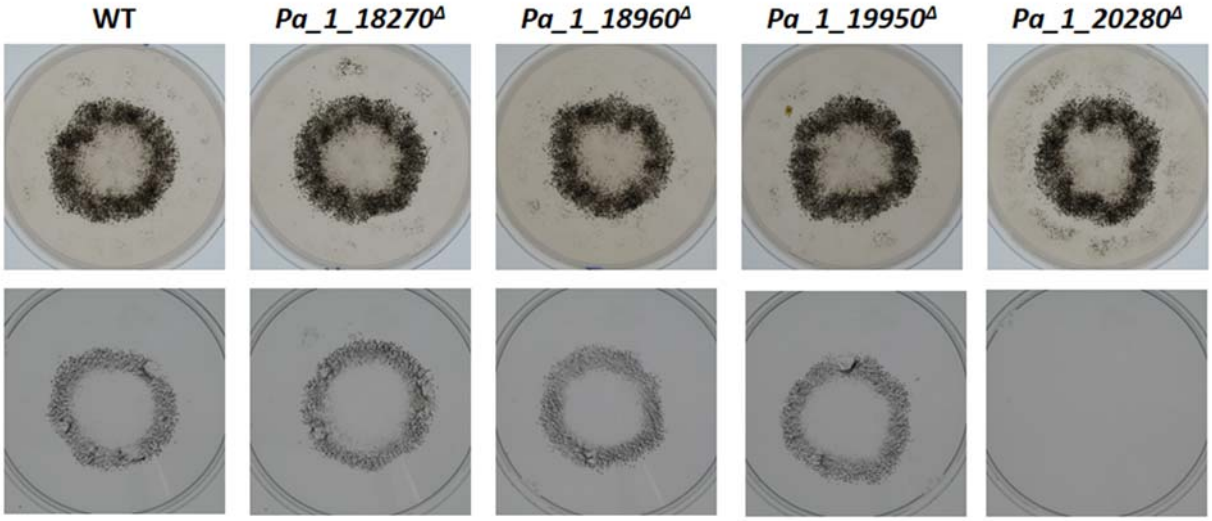

Figure S3 Fertility of agglutinin-like mutants. Top row: Petri plate of typical crosses of the indicated wild type and mutants. Bottom row: cover of the plates where expelled ascospores accumulate. While the *Pa_1_20280*$^{\Delta}$ mutant differentiates normal-looking fruiting bodies that contain ascospores, none are ejected on the plate cover.

Table S1 Number of genes for p-value computing.

Type of genes	Up-regulated in *mat+*	Up-regulated in *mat-*
Total number of genes	63	131
Total number of analyzed genes	61	127
Encoding protein with predicted mitochondrial localization	20	14
Encoding protein with predicted extracellular localization	7	47

Tables S2-S3
Available for download as Excel files at http://www.genetics.org/lookup/suppl/doi:10.1534/genetics.113.159988/-/DC1

Table S2 Polymorphisms between S *mat+* and S *mat-*

Table S3 Expression- and p-values of the 194 genes not controlled by the mating type genes and differentially expressed between *mat+* and *mat-* strains. Fold change (FC), adjusted p-value (p-value) and the binary logarithm of the arithmetic mean of compared intensities (A) are indicated for the 194 genes and for each comparison (*mat+ vs mat-, fpr1$^-$ vs fmr1$^-$, mat+ vs fpr1$^-$* and *mat- vs fmr1$^-$*).

Table S4 Annotation of the 194 genes not controlled by the mating-type genes and differentially expressed between *mat+* and *mat-* strains.

Gene number	Locus	PFAM domain	Putative Function	FC
FMR1	Chrm1	HMG-box	FMR1	-13.91
Pa_1_10350	Chrm1	Glyco_hydro_38, Alpha-mann_mid, Glyco_hydro_38C	Glycoside Hydrolase Family 38	-3.61
nad3	mito		NADH-ubiquinone oxidoreductase chain3	-3
Pa_4_1433	Chrm4	no PFAM matches	conserved protein of unknown function	-2.64
Pa_1_6014	Chrm1	no PFAM matches	putative protein of unknown function specific to Pa	-2.62
nad2	mito		NADH-ubiquinone oxidoreductase chain3	-2.53
Pa_7_15	Chrm7	Chitin bind 3	conserved protein of unknown function	-2.46
Pa_6_11500	Chrm6	Pec_lyase_C	Polysaccharide Lyase Family 1	-2.13
Pa_7_140	Chrm7	AAA, HAD, UPRTase	conserved protein of unknown function	-2.12
Pa_1_13200	Chrm1	DUF3328	conserved protein of unknown function	-2.12
Pa_2_13480	Chrm2	DUF1996	conserved protein of unknown function	-2.08
Pa_1_11070	Chrm1	Glyco hydro 45	Glycoside Hydrolase Family 45	-2.08
Pa_3_10430	Chrm3	no PFAM matches	conserved protein of unknown function	-2.08
Pa_5_7010	Chrm5	no PFAM matches	conserved protein of unknown function	-2.07
Pa_2_13420	Chrm2	DUF3984	conserved protein of unknown function	-2.05
Pa_1_21290	Chrm1	HgmA	homogentisate 1,2-dioxygenase	-1.99
Pa_5_2770	Chrm5	no PFAM matches	conserved protein of unknown function	-1.99
Pa_6_6600	Chrm6	Peptidase_C14	Caspase	-1.91
Pa_3_9740	Chrm3	no PFAM matches	conserved protein of unknown function	-1.91
Pa_6_5020	Chrm6	no PFAM matches	conserved protein of unknown function	-1.9
Pa_5_11630	Chrm5	Glyco_hydro_61	Glycoside Hydrolase Family 61	-1.87
Pa_1_9990	Chrm1	Ank_2	conserved protein of unknown function	-1.83
Pa_5_1860	Chrm5	Pec_lyase_C	Polysaccharide Lyase Family 1	-1.82
Pa_7_120	Chrm7	MFS_1	siderophore iron transporter	-1.82
Pa_7_3060	Chrm7	Radical_SAM, Fer4_14	INF-inducible and antiviral protein	-1.8
Pa_3_11180	Chrm3	Retrotrans_gag, zf-CCHC	gag protein	-1.73
Pa_5_1000	Chrm5	Abhydrolase_2	Carbohydrate Esterase Family 1	-1.71
Pa_5_3730	Chrm5	no PFAM matches	Glycoside Hydrolase Family 79	-1.7
Pa_7_6040	Chrm7	no PFAM matches	carbohydrate-binding module family 1 protein	-1.69

Pa_4_4315	Chrm4	no PFAM matches	conserved protein of unknown function	-1.67
Pa_0_1370	Chrm7	Glyco_hydro_62	Glycoside Hydrolase Family 62	-1.66
Pa_2_13540		no PFAM matches	conserved protein of unknown function	-1.62
Pa_1_6300	Chrm1	Sod_Cu	Cu,Zn superoxide dismutase-like protein	-1.59
Pa_0_130	Chrm6	PBP	protease inhibitor	-1.57
Pa_7_3510	Chrm7	no PFAM matches	conserved protein of unknown function	-1.56
Pa_0_1360	Chrm7	Glyco_hydro_43	Glycoside Hydrolase Family 43	-1.55
Pa_1_16380	Chrm1	Amidase	glutamyl-tRNA(Gln) amidotransferase subunit A	-1.55
Pa_5_245	Chrm5	Carb_bind	non-anchored cell wall protein 3	-1.55
Pa_7_3390	Chrm7	Glyco_hydro_61	Glycoside Hydrolase Family 61	-1.53
Pa_3_190	Chrm3	Glyco_hydro_61	Glycoside Hydrolase Family 61	-1.52
Pa_2_10280	Chrm2	Glyco_hydro_10	Glycoside Hydrolase Family 10	-1.52
Pa_5_13075	Chrm5	no PFAM matches	putative protein of unknown function specific to Pa	-1.52
Pa_3_2620	Chrm3	Glyco_hydro_2_N, Glyco_hydro_2, Glyco_hydro_2_C	Glycoside Hydrolase Family 2	-1.51
Pa_7_5030	Chrm7	Glyco_hydro_61	Glycoside Hydrolase Family 61	-1.51
Pa_4_4920	Chrm4	no PFAM matches	carbohydrate-binding module family 1 protein	-1.5
Pa_7_1080	Chrm7	O-FucT	alternative oxidase	-1.5
Pa_1_17160	Chrm1	Lipase_GDSL	Lipase, GDSL-like protein	-1.49
Pa_7_11630	Chrm7	FAD_binding_4, BBE	oxidase	-1.49
Pa_5_3920	Chrm5	HET	heterokaryon incompatibility protein	-1.48
Pa_6_10770	Chrm6	Sugar_tr	Sugar transporter	-1.48
Pa_5_10750	Chrm5	NPP1	necrosis inducing factor	-1.48
Pa_7_500	Chrm7	SGL, DUF4394	putative carbonic anhydrase protein	-1.48
Pa_6_6610	Chrm6	CHAT	conserved protein of unknown function	-1.47
Pa_7_9790	Chrm7	WSC	related to beta-1,3 exoglucanase	-1.47
Pa_1_13110	Chrm1	HET	heterokaryon incompatibility protein	-1.47
Pa_1_16500	Chrm1	zf-C2H2_4, zf-C2H2	conserved protein of unknown function	-1.47
Pa_2_1700	Chrm2	Glyco_hydro_61	Glycoside Hydrolase Family 61	-1.46
Pa_0_1460	Chrm7	Glyco_hydro_43	Glycoside Hydrolase Family 43	-1.45
Pa_4_4190	Chrm4	Lactonase	carboxymuconate cyclase	-1.45

Pa_5_9310	Chrm5	Glyco_hydro_3, Glyco_hydro_3_C	Glycoside Hydrolase Family 3	-1.45
Pa_1_6675	Chrm1	no PFAM matches	putative protein of unknown function specific to Pa	-1.44
Pa_1_20090	Chrm1	NUDIX	nudix hydrolase	-1.44
Pa_2_4280	Chrm2	FAD_binding_4, BBE	reticuline oxidase precursor	-1.43
Pa_7_10520	Chrm7	Glyco_hydro_1	Glycoside Hydrolase Family 1	-1.43
Pa_4_5620	Chrm4	no PFAM matches	conserved protein of unknown function	-1.42
Pa_2_7040	Chrm2	Glyco_hydro_61	Glycoside Hydrolase Family 61	-1.42
Pa_2_13520	Chrm2	Lipase_3	Lipase family protein	-1.41
Pa_1_21560	Chrm1	AAA	ATPase	-1.41
Pa_7_8610	Chrm7	DUF1762	conserved protein of unknown function	-1.41
Pa_2_4530	Chrm2	no PFAM matches	putative protein of unknown function specific to Pa	-1.41
Pa_4_1400	Chrm4	no PFAM matches	putative protein of unknown function specific to Pa	-1.41
Pa_4_3517	Chrm4	no PFAM matches	PaMt1	-1.41
Pa_3_3700	Chrm3	FKBP_C	similar to FK506-binding protein 1B of N. crassa	-1.41
Pa_1_8450	Chrm1	no PFAM matches	conserved protein of unknown function	-1.4
Pa_5_8940	Chrm5	Glyco_hydro_61, CBM_1	Glycoside Hydrolase Family 61	-1.39
Pa_1_21740	Chrm1	FtsJ	FtsJ-like methyltransferase family protein	-1.39
Pa_2_13780	Chrm2	Peptidase S28	serine protease	-1.38
Pa_1_19650	Chrm1	IBN_N, HEAT_EZ	importin subunit beta-1	-1.38
Pa_1_880	Chrm1	Pro_dh	mitochondrial proline oxidase precursor	-1.38
Pa_6_11690	Chrm6	RdRP	RNA-dependent RNA polymerase 1	-1.38
Pa_2_9990	Chrm2	Fungal_trans	Fungal specific transcription factor	-1.38
Pa_3_2970	Chrm3	DUF4419	conserved protein of unknown function	-1.38
Pa_7_4520	Chrm7	Peptidase_S8, PA, DUF1034	protease	-1.38
Pa_7_5610	Chrm7	ABC_membrane, ABC_tran	heavy metal tolerance protein precursor	-1.37
Pa_7_4840	Chrm7	Propep_M14, Peptidase_M14	carboxypeptidase	-1.37
Pa_7_4620	Chrm7	Asp	aspartic protease	-1.37
Pa_1_21080	Chrm1	Aldo_ket_red	reductase	-1.37

Pa_1_24620	Chrm1	SET	putative mannose-6-phosphate isomerase-like protein	-1.37
Pa_6_9660	Chrm6	no PFAM matches	conserved protein of unknown function	-1.37
Pa_6_1010	Chrm6	Dak1, Dak2	Dihydroxyacetone kinase	-1.36
Pa_4_1440	Chrm4	no PFAM matches	putative integral membrane protein	-1.35
Pa_7_4720	Chrm7	E1-E2_ATPase, Hydrolase	type IB cation-transporting ATPase	-1.34
Pa_5_10380	Chrm5	Glyco_hydro_43	Glycoside Hydrolase Family 43	-1.33
Pa_7_4780	Chrm7	GMC_oxred_N, GMC_oxred_C	GMC oxidoreductase	-1.33
Pa_5_3370	Chrm5	NACHT, WD40	HET containing-domain vegetative incompatibility protein	-1.33
Pa_4_9760	Chrm4	no PFAM matches	cellobiose dehydrogenase	-1.32
Pa_1_12370	Chrm1	HisG	ATP phosphoribosyltransferase	-1.32
Pa_3_6760	Chrm3	no PFAM matches	conserved protein of unknown function	-1.32
Pa_6_7150	Chrm6	HLH	Protein similar to Allergen Fus c 3 of Fusarium culmorum	-1.32
Pa_4_3516	Chrm4	no PFAM matches	conserved protein of unknown function	-1.31
Pa_0_1320	Chrm2	no PFAM matches	Glycoside Hydrolase Family 79	-1.31
Pa_6_11680	Chrm6	Meth_synt_2	5-methyltetrahydropteroyltriglutamate-homocysteine methyltransferase	-1.31
Pa_0_720	Chrm2	SET	putative mannose-6-phosphate isomerase-like protein	-1.31
Pa_1_1170	Chrm1	not in the database	not in the database	-1.3
Pa_3_1630	Chrm3	no PFAM matches	conserved protein of unknown function	-1.3
Pa_5_11240	Chrm5	Esterase	Carbohydrate Esterase Family 1	-1.3
Pa_4_8680	Chrm4	Glucosamine_iso	glucosamine-6-phosphate deaminase	-1.3
Pa_1_8470	Chrm1	PRA1	prenylated Rab acceptor	-1.29
Pa_4_3510	Chrm4	no PFAM matches	conserved protein of unknown function	-1.28
Pa_1_21900	Chrm1	Glyco_hydro_61	Glycoside Hydrolase Family 61	-1.28
Pa_3_7480	Chrm3	Asparaginase_2	asparaginase	-1.28
Pa_6_30	Chrm6	Rhodanese	Thiosulfate sulfurtransferase	-1.27
Pa_3_9090	Chrm3	Ribosomal_L15e	cytosolic 60S ribosomal protein Rpl15	-1.27
Pa_6_9930	Chrm6	no PFAM matches	ino80 chromatin remodeling complex protein	-1.27
Pa_1_18590	Chrm1	no PFAM matches	conserved protein of unknown function	-1.27
Pa_4_1480	Chrm4	Inhibitor_I9, Peptidase_S8	Alkaline serine protease	-1.25

Pa_3_8450	Chrm3	Ribosomal_L27e	cytosolic 60S ribosomal protein Rpl27	-1.24
Pa_3_8520	Chrm3	no PFAM matches	IDC1	-1.24
Pa_1_14940	Chrm1	WD40	Pre-rRNA-processing protein	-1.24
Pa_1_18710	Chrm1	no PFAM matches	zinc finger protein	-1.23
Pa_2_13130	Chrm2	Aldo_ket_red	voltage-gated potassium channel subunit beta	-1.23
Pa_1_10320	Chrm1	Ribosomal_L10, Ribosomal_60S	cytosolic 60S ribosomal protein RplP0	-1.23
Pa_3_4070	Chrm3	no PFAM matches	potassium voltage-dependent transporter	-1.23
Pa_7_11540	Chrm7	Ribosomal_L30_N, Ribosomal_L30	cytosolic 60S ribosomal protein Rpl7	-1.22
Pa_0_980	Chrm2	no PFAM matches	putative thymidylate kinase protein	-1.21
Pa_1_7180	Chrm1	Glyco_hydro_47	Glycoside Hydrolase Family 47	-1.21
Pa_5_7110	Chrm5	DUF1857	conserved protein of unknown function	-1.19
Pa_2_13940	Chrm2	Pkinase	meiotic mRNA stability protein kinase	-1.19
Pa_4_7880	Chrm4	no PFAM matches	putative protein of unknown function specific to Pa	-1.16
Pa_4_4640	Chrm4	AMP-binding, PP-binding	peptide synthase	-1.15
Pa_1_12440	Chrm1	no PFAM matches	transcription factor orthologous to ace1	-1.13
Pa_3_6780	Chrm3	Citrate_synt	mitochondrial citrate synthase CIT1	1.17
Pa_1_740	Chrm1	NIF	mitochondrial import inner membrane translocase subunit tim-50 precursor	1.17
Pa_3_2600	Chrm3	Ldh_1_N, Ldh_1_C	mitochondrial malate dehydrogenase	1.19
Pa_6_2600	Chrm6	PEMT	phosphatidylethanolamine N-methyltransferase	1.19
Pa_3_7700	Chrm3	ATP-grasp_2, Ligase_CoA	mitochondrial succinyl-CoA ligase [GDP-forming] beta-chain precursor	1.19
Pa_1_13750	Chrm1	GCV_T, GCV_T_C	mitochondrial glycine cleavage system T protein	1.19
Pa_3_1040	Chrm3	no PFAM matches	putative integral membrane protein	1.2
Pa_1_17080	Chrm1	Polyketide_cyc2	putative polyketide cyclase dehydrase protein	1.21
Pa_3_9400	Chrm3	GrpE	mitochondrial GrpE protein homolog precursor	1.21
Pa_7_1560	Chrm7	SQS_PSY	mitochondrial squalene/phytoen synthase	1.21
Pa_5_5200	Chrm5	zf-Apc11	anaphase-promoting complex subunit	1.22
Pa_7_6410	Chrm7	Peptidase_M16, Peptidase_M16C	mitochondrial-processing peptidase subunit alpha, mitochondrial precursor	1.23

Pa_1_23270	Chrm1	Abhydrolase_1	homoserine O-acetyltransferase	1.23
Pa_2_6200	Chrm2	GCV_H	mitochondrial glycine cleavage system H protein	1.25
Pa_1_5780	Chrm1	FMO-like	monooxygenase-like protein	1.26
Pa_1_8920	Chrm1	Fer2_3, Fer4_17	mitochondrial succinate dehydrogenase [ubiquinone] iron-sulfur subunit precursor	1.28
Pa_1_6520	Chrm1	Peptidase_M16, Peptidase_M16_C	mitochondrial-processing peptidase subunit beta precursor	1.28
Pa_1_6960	Chrm1	peroxidase	mitochondrial cytochrome c peroxidase precursor	1.29
Pa_7_11550	Chrm2	Fe-S_biosyn	mitochondrial iron sulfur assembly protein	1.29
Pa_5_7360	Chrm5	ABC_membrane, ABC_tran, ATM1	mitochondrial iron-sulfur clusters transporter	1.31
Pa_7_3640	Chrm7	no PFAM matches	conserved protein of unknown function	1.32
Pa_2_11220	Chrm2	DUF3317	conserved protein of unknown function	1.32
Pa_6_5140	Chrm6	Mito_carr	mitochondrial precursor of phosphate carrier protein	1.33
Pa_4_7280	Chrm4	DOPA_dioxygen	DOPA-like protein	1.33
Pa_7_6100	Chrm7	no PFAM matches	conserved protein of unknown function	1.34
Pa_7_760	Chrm7	IDO	indoleamine 2,3-dioxygenase	1.35
Pa_2_12610	Chrm2	ICL	Isocitrate lyase	1.35
Pa_4_750	Chrm4	CFEM	conserved protein of unknown function	1.38
Pa_7_9760	Chrm7	Rdx	selenoprotein domain protein	1.38
Pa_7_2840	Chrm7	Flavin_Reduct	flavoprotein oxygenase	1.38
Pa_6_2810	Chrm6	Cation_efflux	Inorganic ion transporter	1.38
Pa_4_8750	Chrm4	no PFAM matches	related to multidrug resistant protein	1.4
Pa_5_2440	Chrm5	Acetyltransf_8	aerobactin siderophore biosynthesis protein iucB	1.44
Pa_5_7480	Chrm5	Tyrosinase	tyrosinase	1.44
Pa_1_10610	Chrm1	no PFAM matches	conserved protein of unknown function	1.46
Pa_7_6220	Chrm7	ELFV_dehydrog	NAD-specific glutamate dehydrogenase	1.46
Pa_2_1195	Chrm2	no PFAM matches	Putative protein specific to *P. anserina*	1.51
Pa_7_2600	Chrm7	Not in the database	Not in the database	1.54
Pa_2_1415	Chrm2	no PFAM matches	conserved protein of unknown function	1.55
Pa_5_9040	Chrm5	DUF155	conserved protein of unknown function	1.56
Pa_3_11370	Chrm3	no PFAM matches	conserved protein of unknown function	1.56

Pa_4_2250	Chrm4	PPDK_N, PEP-utilizers, PEP-utilizers_C	Phosphoenolpyruvate synthase	1.57
Pa_2_8145	Chrm2	CFEM	conserved protein of unknown function	1.58
Pa_5_6405	Chrm5	no PFAM matches	conserved protein of unknown function	1.59
Pa_4_2305	Chrm4	no PFAM matches	Putative protein specific to *P. anserina*	1.61
Pa_7_4010	Chrm7	HSP20	small heat shock protein	1.65
Pa_1_22370	Chrm1	KGG	conidiation-specific protein 10	1.65
Pa_1_1370	Chrm1	cNMP_binding, F-box, LRR_6	mitochondrial cyclic nucleotide-binding domain-containing protein	1.74
Pa_3_3350	Chrm3	no PFAM matches	conserved protein of unknown function	1.89
Pa_7_5010	Chrm7	Cupin_5 (DUF985)	conserved protein of unknown function	1.9
Pa_3_10590	Chrm3	DUF1768	conserved protein of unknown function	1.96
Pa_6_9940	Chrm6	no PFAM matches	putative protein of unknown funtion	1.96
Pa_2_7590	Chrm2	zf-C3HC4_3	conserved protein of unknown function	2.02
Pa_5_570	Chrm5	K_channel_TID	conserved protein of unknown function	2.04
Pa_1_1230	Chrm1	no PFAM matches	conserved protein of unknown function	2.14
Pa_3_1990	Chrm3		conserved polyketide synthase	2.22
Pa_1_8280	Chrm1	alpha-hel2	conserved protein of unknown function	2.23
Pa_1_20590	Chrm1	HMG-box	FPR1	2.27
Pa_5_11640	Chrm5	ABC_membrane, ABC_tran	conserved mitochondrial ABC transporter	2.34
Pa_1_30	Chrm1	no PFAM matches	protein similar to TmpA of Emericella nidulans	2.35
Pa_5_820	Chrm5	no PFAM matches	conserved protein of unknown function	2.49
Pa_6_540	Chrm6	no PFAM matches	conserved protein of unknown function	2.61
Pa_4_9360	Chrm4	FBPase	fructose-1,6-bisphosphatase	2.67

Table S5 Genes highly differentially expressed in S *mat+* and S *mat-* and whose expression is not under the control of the mating type

CDS	Locus	Putative Function	Affected pathway	fold change S *mat+* versus S *mat-*
nad1	mito	NADH-ubiquinoneoxidoreductasechain 1	respiration	-4.25
nad2	mito	NADH-ubiquinoneoxidoreductasechain 2	respiration	-2.53
nad3	mito	NADH-ubiquinoneoxidoreductasechain 3	respiration	-3
Pa_1_1230	chrm1	Putative protein of unknown function		2.14
Pa_1_30	chrm1	Putative protein similar to the membrane oxidoreductaseTmpA of Emericellanidulans	sexual/asexual development?	2.35
Pa_1_3100	chrm1	Putative oxidoreductase	???	-2.16
Pa_1_5700	chrm1	Potassium transporter Hak-1		-2.4
Pa_1_6014	chrm1	Putative protein of unknown function		-2.62
Pa_1_8280	chrm1	Putative protein of unknown function		2.23
Pa_1_11070	chrm1	Putative Glycoside Hydrolase Family 45 (endoglucanase)	Sugar polymermetabolism	-2.08
Pa_1_13200	chrm1	Putative protein of unknown function		-2.12
Pa_1_1490	chrm1	Putative sorbitol dehydrogenase	pentose metabolism	-2.13
Pa_1_18670	chrm1	Putative protein of unknown function		3.43
Pa_1_19170	chrm1	Putative protein of unknown function		2.54
Pa_1_20140	chrm1	Putative protein of unknown function		2.77
Pa_1_21970	chrm1	Putative GMC oxidoreductase: peroxisomal alcohol oxidase (AOD)	Methanol metabolism	-2.6
Pa_1_22300	chrm1	Putative glycine dehydrogenase	glycine metabolism, serine & threonine metabolism	2.03
Pa_0_1080	chrm2	Putative inositoloxygenase	Inositol phosphate metabolism, Ascorbate and aldarate metabolism	-2.01
Pa_2_11120	chrm2	Putative NADP-dependentmalatedehydrogenase	Pyruvate metabolism	2.08
Pa_2_13420	chrm2	Putative protein of unknown function		-2.05
Pa_2_13480	chrm2	Putative protein of unknown function		-2.08
Pa_2_80	chrm2	Putative transporter protein similar to C11D3.06 of Schizosaccharomyces pombe		-2.52
Pa_2_8150	chrm2	Putative protein of unknown function		-2.15

Pa_3_130	chrm3	Putative protein of unknown function		-2.11
Pa_3_830	chrm3	Putative Carbohydrate EsteraseFamily 1	Sugar polymermetabolism	-2.25
Pa_3_1990	chrm3	Putative polyketide synthase	Secondary metabolism	2.22
Pa_3_5600	chrm3	Putative protein of unknown function	Pseudogene ?	-2.05
Pa_4_230	chrm4	Putative oxidoreductase	???	2.04
Pa_4_80	chrm4	Putative methyltransferase	Secondary metabolism?	2.37
Pa_4_3860	chrm4	Putative alpha/beta hydrolase	???	2.09
Pa_4_4560	chrm4	Putative zeaxanthinepoxidase	???	-2.15
Pa_4_5280	chrm4	Putative Beta-lactamase	???	-2.09
Pa_4_9360	chrm4	Putative fructose-1,6-bisphosphatase	Sugar metabolism	2.67
Pa_4_9550	chrm4	Putative protein of unknown function		-2.07
Pa_5_570	chrm5	Putative protein of unknown function		2.04
Pa_5_820	chrm5	Putative protein of unknown function		2.49
Pa_5_1550	chrm5	Putative protein of unknown function		-2
Pa_5_12470	chrm5	Putative protein of unknown function		2.36
Pa_5_7010	chrm5	Putative protein of unknown function		-2.07
Pa_6_11500	chrm6	Putative Polysaccharide Lyase Family 1	Sugar polymermetabolism	-2.13
Pa_6_540	chrm6	Putative protein of unknown function		2.61
Pa_6_6730	chrm6	Putative protein of unknown function		-2.17
Pa_7_9690	chrm7	Putative protein-S-isoprenylcysteine O-methyltransferase	post-translational modification of proteins	2.95
Pa_7_140	chrm7	Putative protein of unknown function with hydolase and aphosphoribosyltransferase domains	???	-2.12
Pa_7_15	chrm7	Putative protein of unknown function with chitin binding domain		-2.46
Pa_7_950	chrm7	Putative protein of unknown function with transmembrane domain (HPP superfamily)		2.24